GEOLOŠKI ZAVOD SLOVENIJE
Dimičeva ulica 14, 1001 Ljubljana

Geotechnical, Geological, and Seismological (GG&S) Evaluations for the New Nuclear Power Plant at the Krško Site (NPP Krško II)

Paleoseismological investigations of the Libna fault. Trench in Stari Grad.

LJUBLJANA, November 2008

Project	Geotechnical, Geological, and Seismological (GG&S) Evaluations for the New Nuclear Power Plant at the Krško Site (NPP Krško II)
Phase	1st
Contract:	Consortium agreement 1130-167/07
INVESTOR:	Gen-Energija, d.o.o.
Consortium Share of Supplies:	Tasks: 4.3.1.c, 4.3.1.c1, 4.3.1.d
Consortium partners	BRGM, GeoZS, IRSN, ZAG
Responsible for Consortium leader: BRGM Project leader	dr. Behrooz Bazargan Sabet
Responsible for Geološki zavod Slovenije director	dr. Marko Komac
Place	Ljubljana
Date	27.11.2008
Arch. No.	J-II-30d/b6b-3/6-b

Contributors

Miloš Bavec; GeoZS
Stephane Baize, IRSN
Dragomir Skaberne, GeoZS
Jernej Jež, GeoZS

Responsible :	GeoZS	Miloš Bavec
Reviewer:	BRGM	Guillaume Bertrand
Approbation;	IRSN	Oona Scotti

KEY WORDS: NPP Krško II, paleoseismological trench, Libna fault, logging

List of contents

APENDICES

1. ^{14}C dating report. Beta Analytic; D. Hood.
2. ^{14}C dating report . Laboratoire de Mesure du Carbone 14; JP.Dumoulin, C.Moreau.
3. OSL dating report. Institut für Geologie, Universität Bern; F. Preusser.
4. Paleontological report (HGI; V. Hajek-Tadesse)
5. Geophysical report (Geoinženiring; M. Car, R. Stopar)

INTRODUCTION

As a part of the project *Geotechnical, Geological and Seismological (GG&S) Evaluations for the New Nuclear Power Plant at The Krško Site (Npp Krško II)* paleoseismological trenching was conducted across the trace of the Libna fault in order to determine the fault's possible recent activity / capability of surface or near-surface rupturing.

The geophysical preliminaries were performed by R. Stopar and M. Car (Geoinženiring d.o.o). Trench preparation, logging, interpretation and report write-up was done collaboratively by S. Baize (IRSN), M. Bavec and D. Skaberne (GeoZS). Field work and logging was assisted by J. Jež (GeoZS) and four students from the Department of Geology, NTF, University of Ljubljana. M. Bavec coordinated the works and edited the report.

For geographic orientation and description of regional geologic features please refer to the tectonic map of Krško basin (this project) that complements the Geologyl report.

TECTONIC AND MORPHOTECTONIC OUTLINE OF THE REGION

Three major groups of structures are present in the Krško Basin area (Figure 1a). The oldest (»Dinaric«) ones exhibit predominantly NW – SE strike, include large folds (several km) and related faults. Dinaric structures observed in the Mesozoic formations and buried by the Neogene deposits are considered of Paleogene age. Some of these Paleogene faults were also reactivated later in the Neogene. The second group of structures (Balaton structures) are observed in the Neogene (and older) rocks. They mostly exhibit the NE – SW (ENE – WSW) strike and correspond to the strike of the Zagreb and Sv. Nedelja faults (and the Mid-Hungarian Zone).
Relief is driven by 2 almost parallel tectonic features (Orlica anticline and Krško syncline). In between, 2 WSW-ENE structures (Orlica fault and Artiče flexure) affect the fold limbs.
We divide the relief between the Orlica and Krško hills, the Artiče plateau, the Krško Syncline plain.
The Orlica hills and the Artiče plateau exhibit older deposits towards the East, and the Orlica hills elevation increases in the same sense.
Regional slope, following this Neogene fold limb, control an incised drainage network into the Artiče plateau. This network is dramatically asymmetric, suggesting a higher uplift to the East during the period of drainage incision (Quaternary).
Crosscutting the Artiče slope (located above Artiče flexure and reverse fault), each stream shows a weakly increasing slope.
These facts are all together consistent and they strongly support a Quaternary uplift of the whole Northern limb of the Artiče flexure.
The area is seismically active. Fig 1b shows locations of the relocated earthquake epicenters for the period 1977-2008 with respect to the major tectonic features of the area. There is no clear correspondence of the seismic activity and the location of the mapped faults.
Fore more informations refer to report: Geotechnical, Geological, and Seismological (GG&S) Evaluations for the New Nuclear Power Plant at the Krško Site (NPP Krško II) Geology – phase 1.

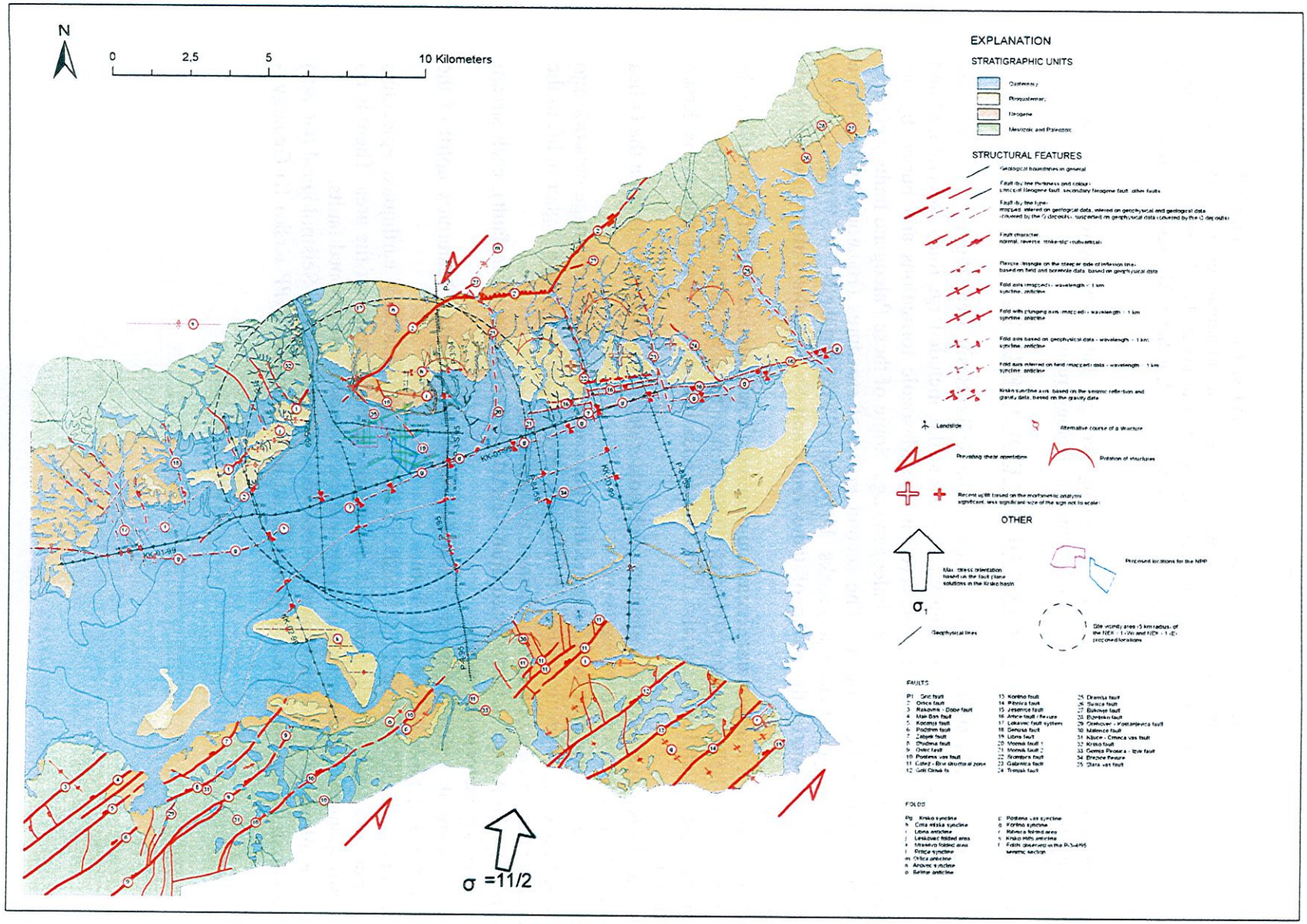

Figure 1a. Tectonic map of Krško basin based on updated 1:25.000 geologic map

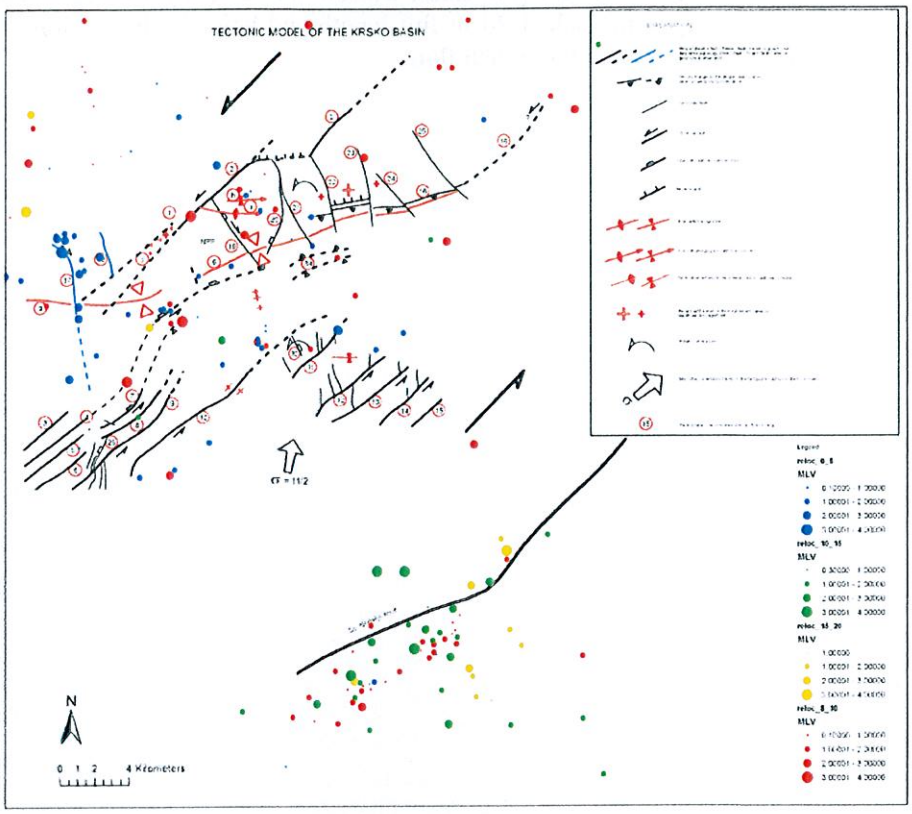

Figure 1b. **Relocated earthquake epicenters plotted over the tectonic model of the Krško basin. .**

TECHNICAL DETAILS

The trench was excavated by excavator and logged between Jan 28th and Feb 1st 2008 following the preliminary geophysical survey. It was placed along the WSW-ENE trending axis between endpoints X=540755.8827; Y=89216.0701 and X=540761.8850; Y=89208.1520 (Gauss-Krueger coordinate system).

The position of the trench was chosen according on the presumed trace of the Libna fault, which was established with the various methods (geological mapping, seismic lines...). Possible recent activity would be proven with displaced and deformed Holocene gravels covering Miocene basement. The significant thickness of the Holocene gravels would cause technical problems during excavation (ground water, possible collapse of the trench wall) so the trenching was performed in the location with relatively thin sheet of gravels.

The axis was moved approximately 10 m NW from the axis of the geophysical preliminaries to enable fieldwork. The trench consisted of the main trench in total length of 52 m at surface and a perpendicular secondary trench in length of 15 meters (Figure 2). Surface width was 6 m. The depth of the trench was 3.7 meters to the NE and 2.3 meters to the SW (Figure 2). This change in depth is due to the slope of the surface. The bottom of the trench was excavated between 40 and 60 cm below the erosional surface between Holocene and Miocene lithologic units and was almost horizontal.

After detailed cleanup the south-eastern wall was equipped for logging in length of 28 m covering the whole height. The slope of the wall was kept at 45 – 90 ° depending on cohesion of the sediment. Before logging the south wall of the trench was marked by measuring grid with cells, 2 m long (lines A, B, C, D, E, F, G, H, I, J, K, L, M, N) and 1m high (lines 1, 2, 3) (Figure 5). The wall was

photographed in sections on axes of vertical grid lines. Mosaic photography was constructed from these sections. The wall was logged in scale 1:20 in full length and height. Observations and some logs were also made on other walls and on the trench floor.

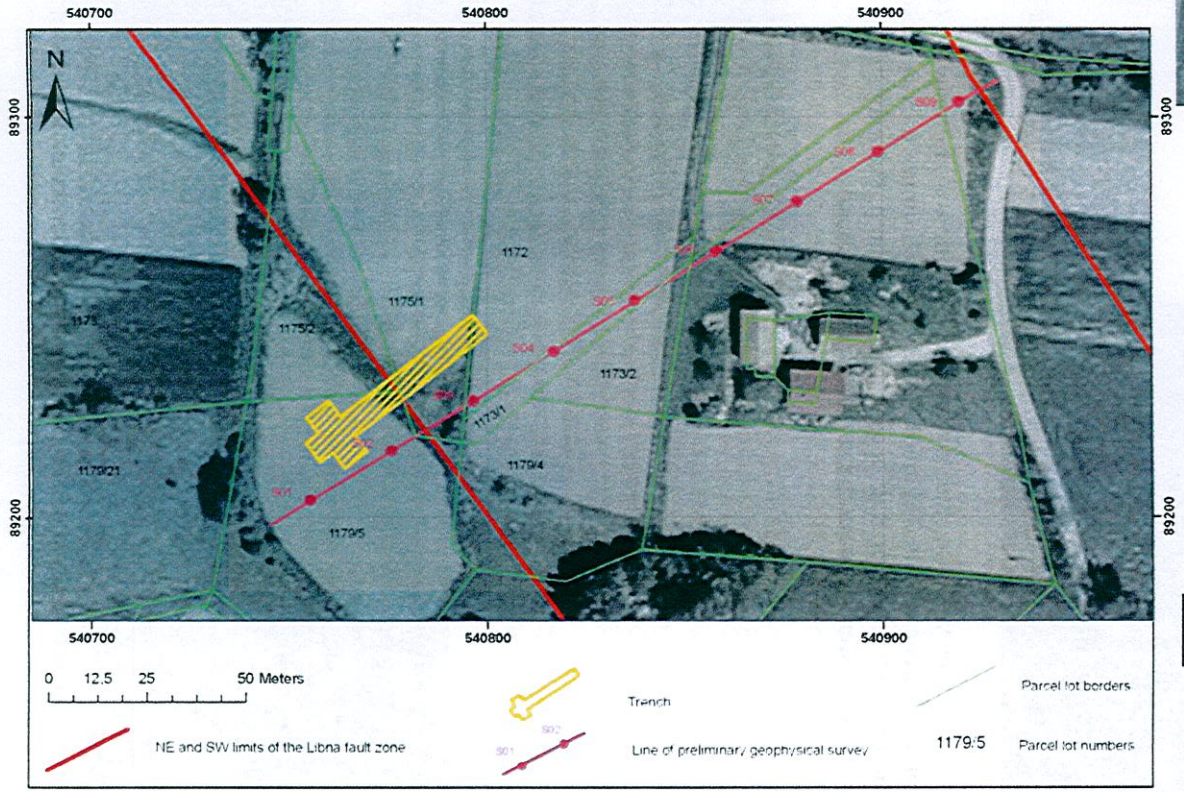

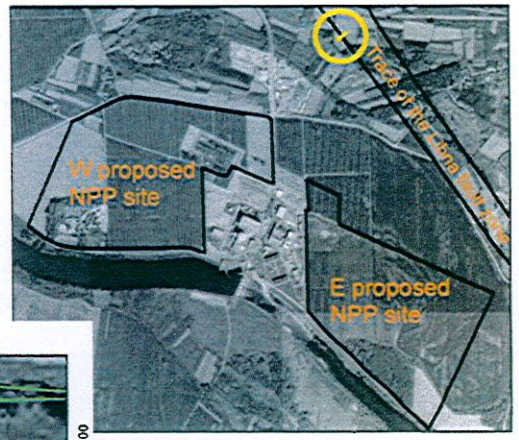

Figure 2. Survey site at Stari grad

Above: Location sketch with trench site indicated in yellow.
Left: Survey site in detail. Gauss - Krueger coordinate system.

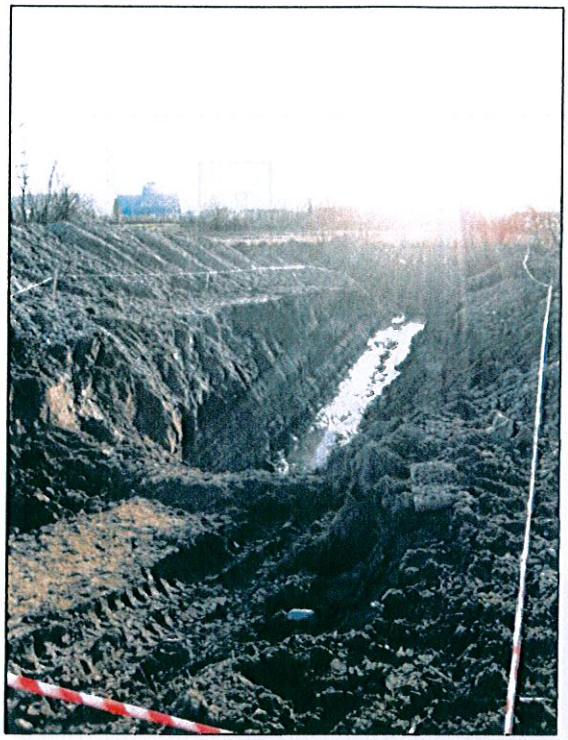

Figure 3. The view over the trench toward the WSW.

Loose gravel in the walls together with significant inflow of groundwater (4 l/s) caused problems with the stability of trench walls (Figure 4). After the preliminary overview a decision was made to keep the southern wall as vertical as possible throughout the survey while other walls including the secondary trench were cleaned and surveyed provisionally.

Figure 4. Groundwater inflow (app. 4 l/s) affected stability of trench wall.

GEOLOGICAL BACKGROUND

GENERAL LITHOLOGY AND STRATIGRAPHY

At Stari Grad trench site the stratigraphy is relatively simple. Atop the sedimentary sequence lie the Holocene fluvial gravels, sands and silts. Along the trench, its thickness varies between 2 and 3.5 meters. Below the Holocene unit, there is the Miocene basement, consisting of massive semi-consolidated silt or clay-silt. The near–horizontal surface between the two units is erosional.
The dip of Miocene layers towards the SE is inferred from regional geology (Brenčič ed., 2006), however a shell-rich layer was observed in the trench dipping toward SSW (198/22).

THE LIBNA FAULT

NW – SE trending fault across Mt. Libna dissecting Plio-Quaternary sediments is named Libna. It was first defined as a buried normal fault with subsided NE block on the Basic geologic map 1 : 100.000 sheet Zagreb (Šikić et al., 1978). Placer (in: Poljak et al., 1997) described several parallel fault (planes) of the same trend in the southern limb of Libna anticline. The fault continuation underneath the Holocene alluvial plain was long unknown. Therefore the last PSHA (Swan et al., 2004) did not pay special attention to this fault. In 2006, during the preliminary geological survey for siting the LILW repository in the vicinity of the existing NPP (Brenčič, ed., 2006), anomalies related to the SE continuance of Libna fault were interpreted in extreme N part of the N – S trending seismic section S1 (This section was during the course of this project evaluated as non reliable due to due to poor quality of the data by the team of experts). Furthermore, horizontal laminae were observed in the core of the VOG-1 borehole drilled in the fault zone in the Upper Miocene deposits (Brenčič, ed., 2006). Considering prevailing south-eastward dip of the strata, observed in the in the construction pit for the NPP, the subhorizontal laminae imply presence of structutural deformation. Repeated remapping in 2006 revealed a single 150 – 300 m wide fault zone (Brenčič, ed., 2006) instead of multiple discrete faults proposed by Placer (in: Poljak, 1997, [78]). One of its western fault planes exhibits normal character with subsided NE block and cuts off the Plioquaternary sediments on the top of Mt.Libna (Placer in: Poljak, 1997, [78]). Libna fault is imaged as an E dipping normal listric fault in the KK-01/99 seismic section (Persoglia (ed), 2000). During the course of this project we realized that such interpretation overestimates the faults importance (see tectonic model report). After the fault was recognized in the S-1 seismic section (Car, 2006; Brenčič ed., 2006) its continuation was also looked for on other seismic sections. During this project we estimated that certain anomaly is also noted on the P-3-4/95 seismic section.

This fault is not to be mistaken with the disproved E-W trending reverse fault in the northern limb of the Libna anticline, also formerly called 'Libna fault' (Placer in: Poljak et al., 1997; Verbič, 1995).

The location of fault trace between Plio-Quaternary gravels and Badenian limestone at the crest of Mt. Libna suggests that the Libna fault, along with the Libna anticline, might have been active during the deposition of the Plio-Quaternary gravels (see tectonic map for geographic explanation). The fact, that not all the faults (fault planes) from the observed NW – SE trending set dissect the lower Plio-Quaternary boundary, implies, that folding of the Libna anticline and the faults formed at that time must have only been active before the deposition of Plio-Quaternary sediments, and that only Libna fault has been active (reactivated?) after (Placer in: Poljak, 1997).

At this stage of the project, we interpret the Libna fault as a fault with relatively subsided NE block with characteristics of both, a normal, and a strike slip fault. No sedimentary deformation or topographic expression in post-Plio-Quaternary sediments is known to be related to the Libna fault. No direct observations of recent activity are known (e.g. notable displacement in the Holocene alluvial plain).

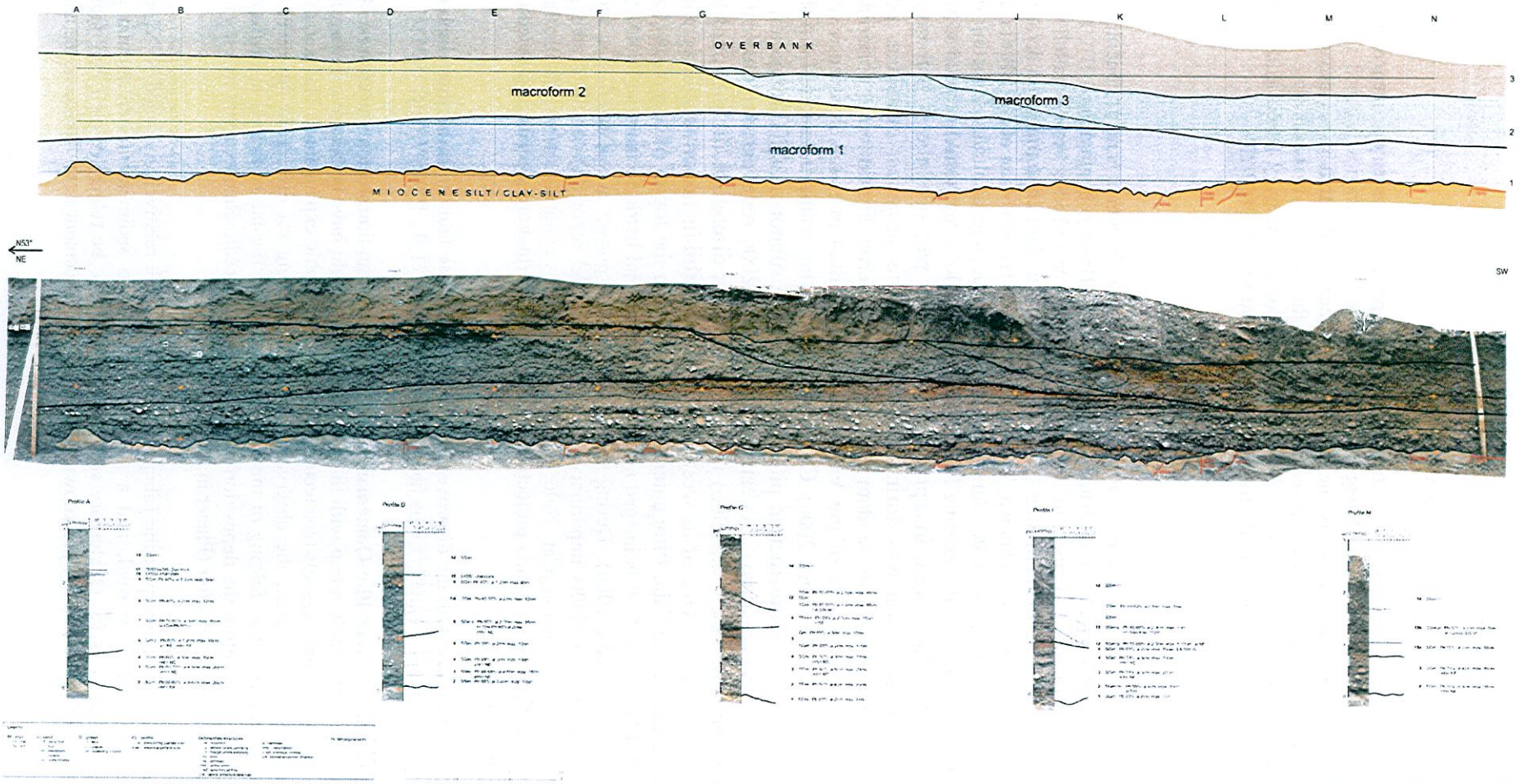

Figure 5. SE trench wall with detailed profiles (below) and sedimentary units key (above)
(For full-size picture see Figure 4 appended to the report.)

PRELIMINARY GEOPHYSICAL SURVEY

Preliminary geophysical survey (appendix 5) was made in the Holocene (historical) alluvial plain, a few hundred meters south of the Libna foothill. The line (200 m long) crossed the whole width of the Libna fault zone in order a) to evaluate thickness of Holocene sediments prior to excavation and more importantly b) to identify potential major deformations at the base of the Holocene fluvial infill. The location of geophysical survey is indicated on Figure 2.

Three methods were foreseen for the survey: refraction seismic survey, active MASW and GPR (ground penetrating radar). However, only refraction seismic survey and MASW were executed (Figure 6), due to elevated water table within the Holocene gravels that obstructed the GPR signal to such an extent that measurements were not possible.

Figure 6. "Landstreamer" acquisition setup for seismic survey across the Libna fault zone

A rough estimate of Holocene infill thickness was attempted by compiling the results of both methods. There were no clear evidence of deformation, yet it was noted that between the points S02 and S05 and especially between S02 and S03 (Figure 7) the Miocene surface is less even if compared to the rest of the profile. For that reason, the decision was made to focus further actions to this part of the fault zone.

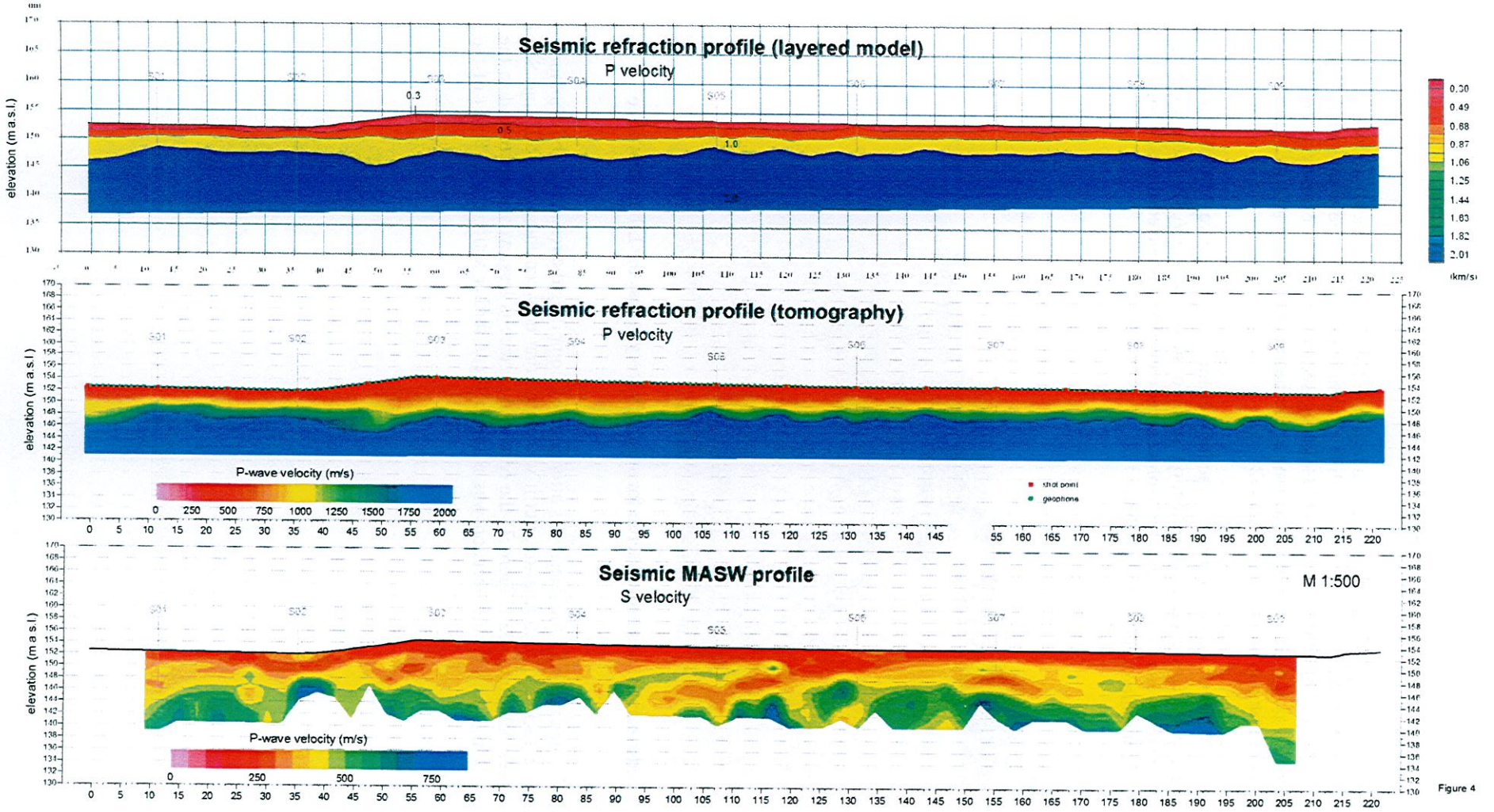

Figure 4

Figure 7: Refraction seismic, and MASW cross sections across the trace of the Libna fault at Stari grad. The direction (right-hand) of the profiles is N69°.

TRENCH LOG

The wall was logged in scale 1:20 in a length of 28 m and up to 3 m height. Main mapped units are outlined on the mosaic photography (Figure 5). Description of main sedimentary units is represented here in respect to five vertical profiles drawn about 6 m apart. Description is based on macroscopic observations.

DESCRIPTION AND INTERPRETATION OF MAIN SEDIMENTARY UNITS

GENERAL DESCRIPTION

The **Miocene base** consists of semi-consolidated silt or clay-silt.

The Miocene sediments are overlain by about 3.5 m thick **unconsolidated Holocene sediments** of fluvial origin. They consist of up to 2.2 m thick **braided-stream deposits** that are overlain by about 1.5 m thick **overbank fine sandy silt**. These sediments were divided into 14 lithological units (figure 4). Carbonate rocks (mostly limestone) prevail in composition of the pebbles, indicating provenience of the Sava River. The channel deposits are divided into three sedimentary macroforms that are at their bases bounded by erosional surfaces.

SEDIMENTARY LOG

Miocene (Pannonian) silt and clay-silt

This layer is very homogeneous. It is very rare to find an evidence of stratification within these grey marls. When found, this is highlighted by an accumulation of shells. At one such spot the in the trench a dip toward SSW (198/22) was observed. The current top surface of this unit is erosional. Together with the facies of upper layers, it is clear that the erosion is of fluvial origin. The most prominent features are the scour marks (25 to 100 cm of amplitude; 10-25 cm of height) (Figure 8). Due to the relative position of steep and gentle slopes, they indicate a clear north-eastward flow.

Figure 8: Example of scour cast at the erosional surface of the Miocene silt and clay-silt / erosional base of the Holocene fluvial sediments. The flow sense to the left (i.e. NE) in fluvial gravels is indicated both by the steeper slope location in the scour cast and the imbrication of flat pebbles.

Holocene braided-stream deposits

The Holocene unit is devided into three sedimentary macroforms (1,2,3) and the overlaying overbank deposits that are further subdivided into lithological units (LU). Denominations and descriptions refer to the Figure 5.

Holocene Macroform 1

The first erosive macroform overlies the Miocene basement and can be divided into five lithological units.

1. Brownish grey massive sandy gravel (SGm). Pebbles occupy 60 % of the sediments. Mean size of pebbles is 2 cm, max. size is 7 cm. The unit is preserved in the depression between G and L. Its max. thickness is up to 30 cm.
2. Grey mostly massive sandy gravel with some indistinct planar cross-bedded at the SE (SGm-(p)). Pebbles occupy 50 % of the sediment, Mean size of pebbles is 3-4 cm, max. size is 30 cm. Imbrication ←NE was observed. The thickness of the unit is about 25 cm.
3. Grey massive sandy gravel (SGm). Pebbles occupy 50 % (70% in places) of the sediment. Mean size of pebbles 4-5 cm, max. size is 20 cm. Imbrication ←NE was observed. The thickness of the unit is about 30 cm.
4. Grey massive sandy gravel (SGm). Pebbles occupy 40-60 % of the sediment. Mean size of pebbles is 3 cm, max. size is 15 cm. Imbrication ←NE was observed. The mean thickness is about 30 cm.
5. Grey and reddish massive sandy gravel (SGm). Pebbles occupy 60 % of the sediment. Mean size of pebbles is 2 cm, max. size 10 is cm. In central part of the trench coarsening upward to massive gravel (Gm) was observed. There pebbles with mean size of 3 cm and max. size 15 cm occupy 80 % of the sediment. The mean thickness is about 35 cm.

Interpretation: The first sedimentary macroform is interpreted as a bar complex composed of five longitudinal bars (lithological units), formed by a braided-style stream, flowing in the direction to the NE (imbrication).

Holocene Macroform 2

The second macroform overlies an erosional surface dipping in the direction to NE and cutting into the first macroform. It is thickening towards the NE, from about 115 cm to about 155 cm (where the lithological units n°5 and n° 4 are respectively entirely and partly eroded). This macroform can be divided into four lithological units in the NE part. Bedding was observed at the NE part of the trench and is getting less distinct (vanishes) toward the SW.

6. Grey massive and trough cross-bedded sandy gravel (SGm). Pebbles occupy 50 % of the sediment. Mean size of pebbles is 2-3 cm, max. size is 15 cm. Imbrication ←NE was observed. Within this unit lenses up to 1m long and up to 15 cm thick of massive gravel (Gm) exist. In these lenses pebbles of mean size around 2 cm occupy 80 % of the sediment. In the NE part of the section we observed transition to planar cross-bedded gravel (Gp) with pebbles occupying 80 % of the sediment. Mean size of pebbles in this sub-unit is 1-2 cm, max. size is 10 cm. Imbrication ←NE was observed and planar cross-bedding dipping to NE. The mean thickness of the whole unit 6 is about 40 cm.
7. Grey massive sandy gravel (SGm). Pebbles occupy 50-60% of the sediment. Mean size of pebbles is 3 cm, max. size is 15 cm. In the upper part, lenses are observed up to 1m long and up to 15 cm thick, consisting of massive gravel (Gm). In these lenses pebbles occupy 80 % of the sediment, their mean size 2 is cm. The mean thickness of the whole unit is about 35 cm.
8. Grey massive sandy gravel (SGm). Pebbles occupy 40-50 % of the sediment, their mean size is 2 cm and max. size is 12 cm. The mean thickness of the unit 8 is about 60 cm.

9. Brownish grey massive sandy gravel (SGm). Pebbles occupy 40 % of the sediment, their mean size is 1-2 cm and max. size is 6 cm. The thickness of the unit is about 15 cm.

Interpretation: The second sedimentary macroform is interpreted as bar complex composed from longitudinal and (maybe) some diagonal bars, formed by a braided-stream flowing in the NE direction (imbrication and planar cross-bedding).

Holocene Macroform 3

The third macroform overlies the second macroform to the NE and the first macroform to the SW, because of the dip of its basal erosional surface. It is mainly composed of coarse-grained gravely sediments, but some fine-grained silty sediments are inclosed.

10. Dark grey nearly black organic rich sandy silt (OrSSi) with charcoal fragments overlies the second macroform. Toward the SW sediment in this layer coarsens and passes to silty sand. The layer's thickness is 5 cm, however it pinches out (or was eroded) in SW part of the section.
11. Grey horizontally laminated fine silty sand (fSiShl) with laminae of coarse sand and thin beds and lenses of sandy gravel up (lenses up to 2 cm thick) form a thin lenticular sand body that is up to 15 cm thick in NE part of the section and it pinches out to SW. Alternative interpretation of this layer could be that it is a part of the overbank sedimentary unit that overlies it.
12. Grey massive and in SW part indistinct planar cross-bedded sandy gravel (SGm-p). Pebbles occupy 50-60 % of the sediment, their mean size is 2-3 cm and max. size is 10 cm. The cross-bedding is dipping to the NE. This lithologic unit overlies the master erosion surface dipping to the SW, and is cutting into sediments of both the second and the first macroform. It incloses smaller lenses of sandy silt (SSi) as well as erosion and accretion surfaces of the lower order, all dipping to the SW.
13. Grey, partly reddish grey massive and planar cross-bedded sandy gravel (SGm-p). Pebbles occupy 40-60 % of the sediment. Pebbles mean size is 2-3 cm and max. size is 7 cm. It overlies erosion surface dipping to the SW, thus cutting off the 12. lithologic unit and cutting into sediments of the second and the first macroform. This lithologic unit can be divided into two parts (13a and 13b) toward the SW, where it is separated by indistinct erosion or lateral accretion surface. Along the erosion surface the 13a, the unit includes lenses of sandy silt up to 1.3 m long and some rib up clasts of sandy silt, up to 55 cm accross. There are also lenses of gravel with pebbles (mean size 1-2 cm; up to 5 cm accross) occupying 80 % of the sediment, that gently dip toward the SW. Pebbles are coated by black Mn oxides in some of those lenses. The sandy gravel is cross-bedded in places. The cross-beds are dipping to SW.

Interpretation: The third macroform is interpreted as channel complex deposited by lateral accretion to the west - south-west. The stream was flowing in a southward direction .
Between 1^{st}-2^{nd} macroforms and 3^{rd} macroform, the stream thus changed its course by about 90°. It was then flowing to the south, cutting a channel into the older sediments.

Overbank sediments of LU10 and LU11 were deposited before the channel was filed by LU12. LU11 filled a small depression on the second macroform.

Holocene overbank deposits

The uppermost lithologic unit, covering the whole section, is the unit consisting of fine - grained overbank deposits.

14. Grey mostly massive, partly horizontally laminated sandy silt (SSim-(l)) on which a thin veneer of recent soil is formed. The unit is about 1.5 m thick.

Interpretation: This lithological unit is interpreted as overbank sediment deposited by more distant stream running on a flood plain formed by older channel deposits.

AGE OF SEDIMENTS

For the holocene unit the age was determined by two independent absolute dating methods in three labs (see table 1 for results and Figure 5 for sampling sites). The organic remains of adequate size were treated at commercial ^{14}C lab (appendix 1), while the small size samples needed more sophisticated approach and were treated at another laboratory (appendix 2). Two samples for OSL age-determination were also analyzed (appendix 3). Results are listed in table below.

^{14}C (Beta Analytic; Darden Hood)

SAMPLE	REMARK	RESULT
SG1	Peat from the gravel unit. Position provisional due to wall collapse - between B1 and B2	sample destroyed
SG5	Wood from the 5cm clay/silt layer below the upper sand unit. Outside gridded part. App 150 cm left (NE) from A.	170±40 (^{14}C yr)
SG9	Charcoal from the N wall. Upper sand unit.	190±40 (^{14}C yr)

^{14}C (Laboratoire de Mesure du Carbone 14; JP.Dumoulin, C.Moreau)

SAMPLE	REMARK	RESULT
SG4	Wood from the 5cm clay/silt layer below the upper sand unit. Outside gridded part. App 3,9 cm left (NE) from A.	225±30 (^{14}C yr)
SG6	Charcoal from the lower gravel unit. Very small sample. 30 cm left and 20 cm down of B3.	8125±30 (^{14}C yr)
SG7	Peat from the »lower« gravel unit. 75 cm left and 35 cm up from C2.	395±30 (^{14}C yr)

OSL (Institut für Geologie, Universität Bern; Frank Preusser)

SAMPLE	REMARK	AGE
SG2	Upper sand/slit layer. 65cm up and 20 cm right of D3	920 ± 1560 yr
SG3	Collapsed sand/silt clast. 30 cm left and 30 cm up of K2	850 ± 190 yr

Table 1. Absolute age dating results of Holocene sediments from the Stari grad trench. Sampling sites are indicated on Figure 5.

Due to methodological limitations we accept the results for SG5, SG9, SG4 and SG 7 as most reliable. We estimate that the age of SG6 was most probably overestimated due to reworking. Due to very low ages of the sediment, the OSL method did not provide results of sufficient quality and should be in this case neglected. We thus interpret the age of the Holocene unit to be around 200 years b.p. for the uppermost layer and around 400 years for the lower layers.

For the Miocene unit the age was determined by paleontological analyses of ostracode fauna (appendix 4). Its stratigraphic age was determined to be at the transition between the Lower, and Mid-Pannonian - C/D *Hungarocypris* zone (stratigraphic division after Piller et al. 2007). In absolute age this is roughly around 10,5 million years b.p. which would in global stratigraphic division correspon to the Lower Tortonian.

STRUCTURAL AND NEOTECTONIC OBSERVATIONS AT THE MIOCENE / HOLOCENE BOUNDARY

All along the trench, we found evidences of fracturing within the Miocene unit. Eleven fractures were prominent enough to enable univocal observation and dip measurement (Figures 5, 9). Because of the absence of clear stratification in the marls, we could not infer the amount of potential displacements and we only found once evidence of slip.

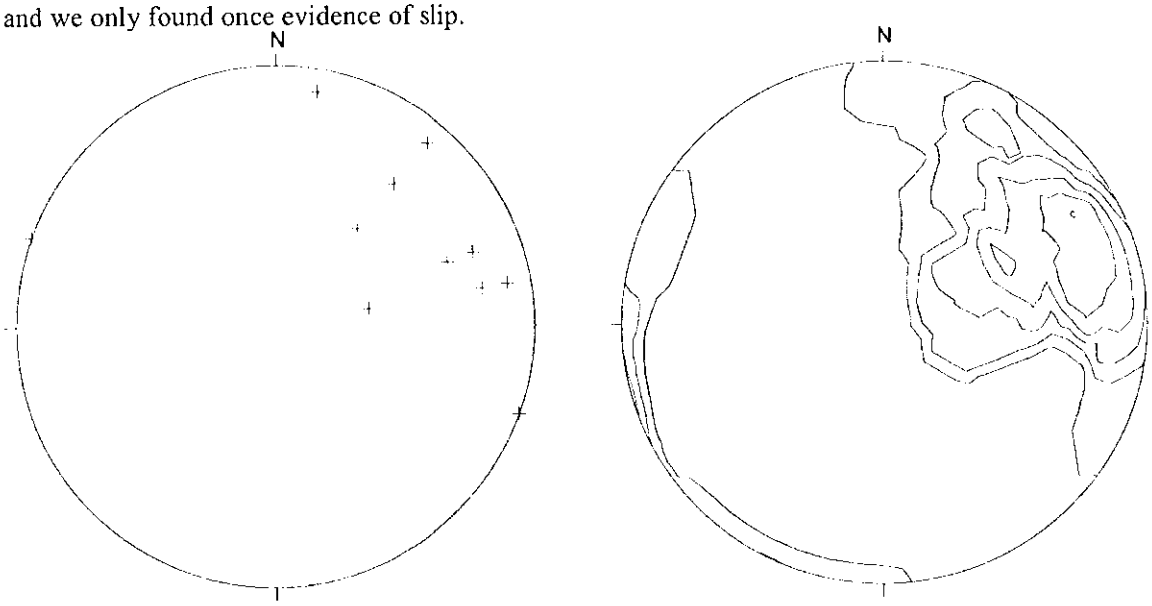

Figure 9. Stereographic projection of fracture poles Equal area, upper hemisphere projection. Left: dip measurements, right: density plot.

Although the number of measurements is too low for statistical treatment, a rough estimate of prevailing strike is possible and does support the hypothesis of direct relation of deformation to the trace of Libna fault zone (NNW-SSE).

The fractures do not exhibit any displacements within the Holocene deposits neither displacement of the Miocene upper erosional surface with an exception of one system. The feature that was observed at the far SW part of the SE wall (the far right deformation shown on Figure 4) may allow an interpretation as being a result of tectonic displacement, not only within the Miocene sediments but also of the Miocene/Holocene boundary. Namely, the irregularity in the erosional surface is oriented opposite to expected scour cast orientation (against the interpreted stream direction). In addition, the erosional surface exhibits a sharp step (5-8 cm high, Figure 10) right above this fracture in Miocene sediments. The system of fractures is prominent enough to be followed across the trench floor to its northern wall. There, 70 cm southwest from the NW wall, the general pattern of the faults suggests an apparent right-lateral kinematics on N150° planes (Figures 11 and 12). The strike-slip motion on these faults is confirmed by the gently north dipping striae on some lustrated planes (Figure 13). This general pattern in the Marls is consistent with the expected trace of the mapped Libna fault.

Along a part of this Miocene/Holocene step, we found that the Miocene marls are "striated" along fault, as we can observe linear "negative" imprints with individual lengths of 10-15 cm (Figure 10). These linear features could be interpreted as grooves made by pebbles. This would mean that the Pleistocene/Holocene gravels could have been displaced along the marls after their deposition, during an offset of the fault. These imprints have a slight plunge to the south (10-15°), which is slightly steeper if compared to the few observed striae in the Miocene sediments (2° to 5°),

Such imprints due to sliding of clasts along a soft rock are known as trailed material indicators (Doblas, 1998) or tapering grooves (Petit and Laville, 1987). We could not observe the tapering shape of the lineation, in order to infer the sense of slip.

The texture of the overlying sediments, as well as the low amplitude of potential displacements, may explain the absence of fracturing or shearing. The Pleistocene gravels have here a large amount of sandy/clay matrix. This "non-shearing" behaviour is known for similar conditions (lithology, saturated or soft sediments), even for larger offsets

There is however, a plausible interpretation of these features that does not include tectonic displacement along the fault after deposition of the Holocene gravel. Since the deformations were found at the far end of the trench, we had a chance of removing in full the Holocene sedimentary sequence at the SW trench wall and see the irregularity also in ground plan (Figure 14). Following its trace in length of app 3 m, it became clear that the step (offset?) in the erosional surface diminishes from 5 - 8 cm to none. The fractured zone below the gravel infill has served as groundwater conductor which is well visible at its upper surface (Figures 10 and 14). From this we infer that it is possible that only groundwater flow caused the selective erosion along deformed thus softened sediment. In that interpretation, deformation continuation since deposition of Holocene sediments is not necessary to explain our observations. No visible deformation in gravel above such erosional feature (a collapse) can have identical explanation as lack of visible deformation in the same material when tectonically deformed.

Figure 10. A sharp step in the Miocene / Holocene erosional boundary before and after the full cleanup of the ground plan.

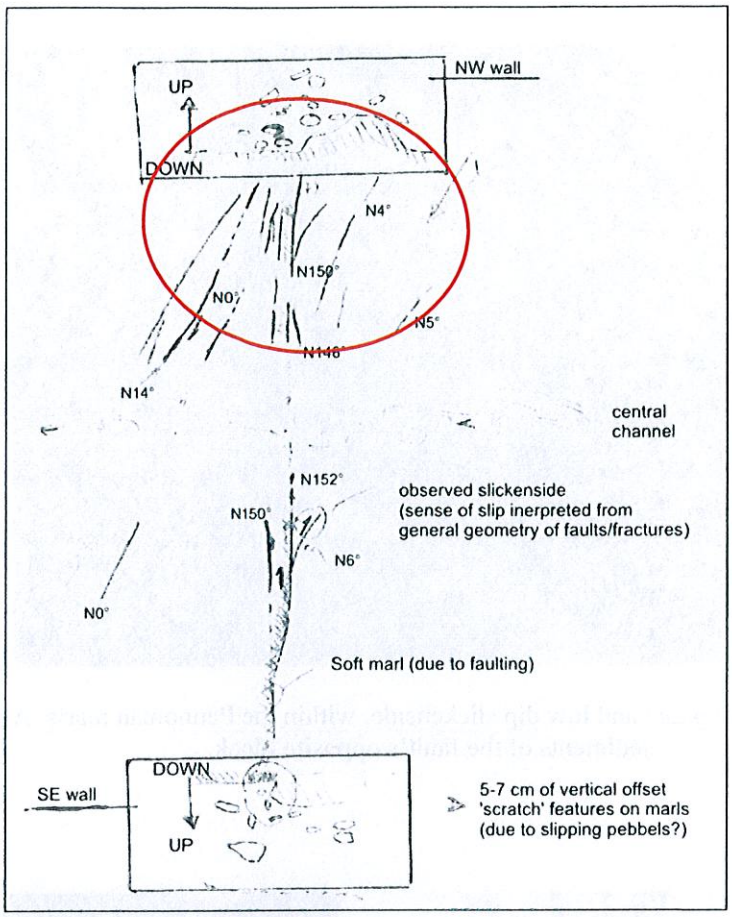

Figure 11: Sketch map of the N150° fault zone in the Miocene sediments. The 2 insets represent the schematic section of the walls at the location of the observed step in the Miocene/Holocene boundary.

Figure 12. Continuation of the N150° system of fractures to the NW trench wall

Figure 13: Lustrated fault plane and low dip slickenside, within the Pannonian marls. After removing sediments of the fault's opposite block.

Figure 14. The irregularity in Miocene /Holocene erosional Boundary after removal of Holocene fluvial sequence from the NW trench wall.

STRUCTURAL INTERPRETATION

These tenuous observations are not conclusive concerning the recent activity of the Libna fault. Faulting within the Miocene sedimentary sequence is a fact, however its continuation into the Holocene fluvial sediments is highly ambiguous. We believe that given the amount of information that we obtained from this survey, two interpretations are equally plausible:

1. The step in the Miocene / Holocene boundary is an erosional feature formed due to enhanced erosion along the faulted and fractured Miocene substratum.
2. The step in the Miocene / Holocene boundary is an offset along one of the fault planes within the Libna fault zone.

CONCLUSIONS

The aim of the paleoseismological survey was to determine possible recent activity of the Libna fault by finding either:

- tectonic displacement within the Holocene fluvial cover or,
- tectonic displacement of the boundary between the Holocene fluvial cover and its Miocene silt / clay - silt substratum.

The results are ambiguous.

Tectonic displacement within the Holocene fluvial sedimentary sequence was not observed. However, the fluvial gravel is only up to 400 years old, so minor displacements may have been overlooked. With a slip rate of 0.1 mm/a (order of magnitude), one can only expect 4 cm of displacement if the Libna fault was active. In addition, such coarse grained and loose sediments may compensate for significant displacements by internal restructuring of the sediment.

Tectonic displacement was also not conclusively observed at the boundary between the Holocene fluvial cover and its Miocene silt / clay - silt substratum. However, at the far SW side of the trench a series of evidences were observed that may equivalently lead to two opposite interpretations. The first interpretation does not include any tectonic displacement after deposition of the Holocene gravel (in historic times). The second interpretation, on the other hand, infers post depositional tectonics.

In order to narrow down the ambiguities we suggest a consideration for paleoseismological trench in the Libna hill or at its foothills where older sediments could have recorded more cumulated deformation if it exists.

REFERENCES

Brenčič, M. (ed.) 2006 : Izvedba terenskih raziskav na potencialnih lokacijah v Republiki Sloveniji, za prostorsko umestitev odlagališča nizko in srednje radioaktivnih odpadkov (NSRAO), v postopku priprave državnega lokacijskega načrta (DLN) za odlagališče NSRAO, 2. faza – začetne terenske raziskave geosfere in hidrosfere potencialna lokacija Vrbina v občini Krško. Končno poročilo. - Konzorcij partnerjev ZAG, GeoZS, ZVV Maribor, Geoinženiring d.o.o.

Car, M., Stopar, R., Giustiniani, M., Accaino, F. 2006: Izvedba terenskih raziskav na potencialnih lokacijah v Republiki Sloveniji, za prostorsko umestitev odlagališča nizko in srednje radioaktivnih odpadkov (NSRAO), v postopku priprave državnega lokacijskega načrta (DLN) za odlagališče NSRAO, 2. faza – začetne terenske raziskave geosfere in hidrosfere potencialna lokacija Vrbina v občini Krško, Sklop 3: Površinske geofizikalne raziskave. – Geoinženiring d.o.o.

Doblas, M. 1998: Slickenside kinematic indicators. - Tectonophysics, 295, 187-197

Persoglia, S. (ed.) 2000: Geophysical research in the surroundings of the Krško NPP (Contract No. 98-0286.00). - European Commission, Directorate general IA, Tacis procurement unit.

Petit J.P. & Laville E. 1987: Morphology and microstructures of hydroplastic slickensides in sandstone. - Geol. Soc. Lond. spec. publ., Conf. Deformation of sediments and sedimentary rocks, N° 29, 107-121.

Piller, W. E., Harzhauser, M. & Mandić, O. (2007): Miocene Central Paratethys stratigraphy - current status and future directions. *Stratigraphy,* vol.4., 151-168.

Poljak, M., Verbič, T., Rižnar, I., Toman, M. & Demšar, M. 1996: Detajlno geološko kartiranje območja Libne pri Krškem in okolice. – 11 str., 19 pril., Arhiv GeoZS, Ljubljana.

Poljak, M., Placer, L., Stojanovič, B. & Rifelj, H. 1997: Geološka reambulacija hriba Libne pri Krškem in okolice. - Unpublished report prepared by the Inštitut za geologijo geotehniko in geofiziko (IGGG), št. dok. ŠGGS15, 21 p.

Verbič, T., 1995, Kvartarni sedimenti v vzhodnem delu Krške kotline: Unpublished report, št. dok. ŠGGS7, 248 p.

Paleoseismological investigations of the Libna fault. Trench in Stari Grad.

Appendix 1

Beta Radiocarbon dating results

FROM: Darden Hood, Director (mailto:mailto:dhood@radiocarbon.com)
(This is a copy of the letter being mailed. Invoices/receipts follow only by mail.)

April 3, 2008

Mr. Milos Bavec
Geological Survey of Slovenia
Dimieeva ulica 14
Ljubljana 1000
Slovenia

RE: Radiocarbon Dating Results For Samples SG5- KK TRENCH, SG9- KK TRENCH

Dear Mr. Bavec:

Enclosed are the radiocarbon dating results for two samples recently sent to us. They each provided plenty of carbon for accurate measurements and all the analyses proceeded normally. As usual, the method of analysis is listed on the report with the results and calibration data is provided where applicable.

As always, no students or intern researchers who would necessarily be distracted with other obligations and priorities were used in the analyses. We analyzed them with the combined attention of our entire professional staff.

If you have specific questions about the analyses, please contact us. We are always available to answer your questions.

Thank you for prepaying the analyses. As always, if you have any questions or would like to discuss the results, don't hesitate to contact me.

Sincerely,

Darden Hood

Mr. Milos Bavec

Report Date: 4/3/2008

Geological Survey of Slovenia

Material Received: 3/4/2008

Sample Data	Measured Radiocarbon Age	13C/12C Ratio	Conventional Radiocarbon Age(*)
Beta - 242030	180 +/- 40 BP	-25.4 o/oo	170 +/- 40 BP

SAMPLE : SG5- KK TRENCH
ANALYSIS : AMS-Standard delivery
MATERIAL/PRETREATMENT : (wood): acid/alkali/acid
2 SIGMA CALIBRATION : Cal AD 1650 to 1890 (Cal BP 300 to 60) AND Cal AD 1910 to 1950 (Cal BP 40 to 0)

Beta - 242031	180 +/- 40 BP	-24.5 o/oo	190 +/- 40 BP

SAMPLE : SG9- KK TRENCH
ANALYSIS : AMS-Standard delivery
MATERIAL/PRETREATMENT : (charred material): acid/alkali/acid
2 SIGMA CALIBRATION : Cal AD 1650 to 1700 (Cal BP 300 to 250) AND Cal AD 1720 to 1820 (Cal BP 230 to 130)
Cal AD 1840 to 1880 (Cal BP 110 to 70) AND Cal AD 1920 to 1950 (Cal BP 40 to 0)

CALIBRATION OF RADIOCARBON AGE TO CALENDAR YEARS

(Variables: C13/C12=-25.4:lab. mult=1)

Laboratory number: **Beta-242030**

Conventional radiocarbon age: **170±40 BP**

2 Sigma calibrated results: **Cal AD 1650 to 1890 (Cal BP 300 to 60) and**
(95% probability) **Cal AD 1910 to 1950 (Cal BP 40 to 0)**

Intercept data

Intercepts of radiocarbon age with calibration curve: Cal AD 1680 (Cal BP 270) and
Cal AD 1770 (Cal BP 180) and
Cal AD 1800 (Cal BP 150) and
Cal AD 1940 (Cal BP 10) and
Cal AD 1950 (Cal BP 0)

1 Sigma calibrated results: Cal AD 1660 to 1690 (Cal BP 280 to 260) and
(68% probability) Cal AD 1730 to 1810 (Cal BP 220 to 140) and
Cal AD 1920 to 1950 (Cal BP 30 to 0)

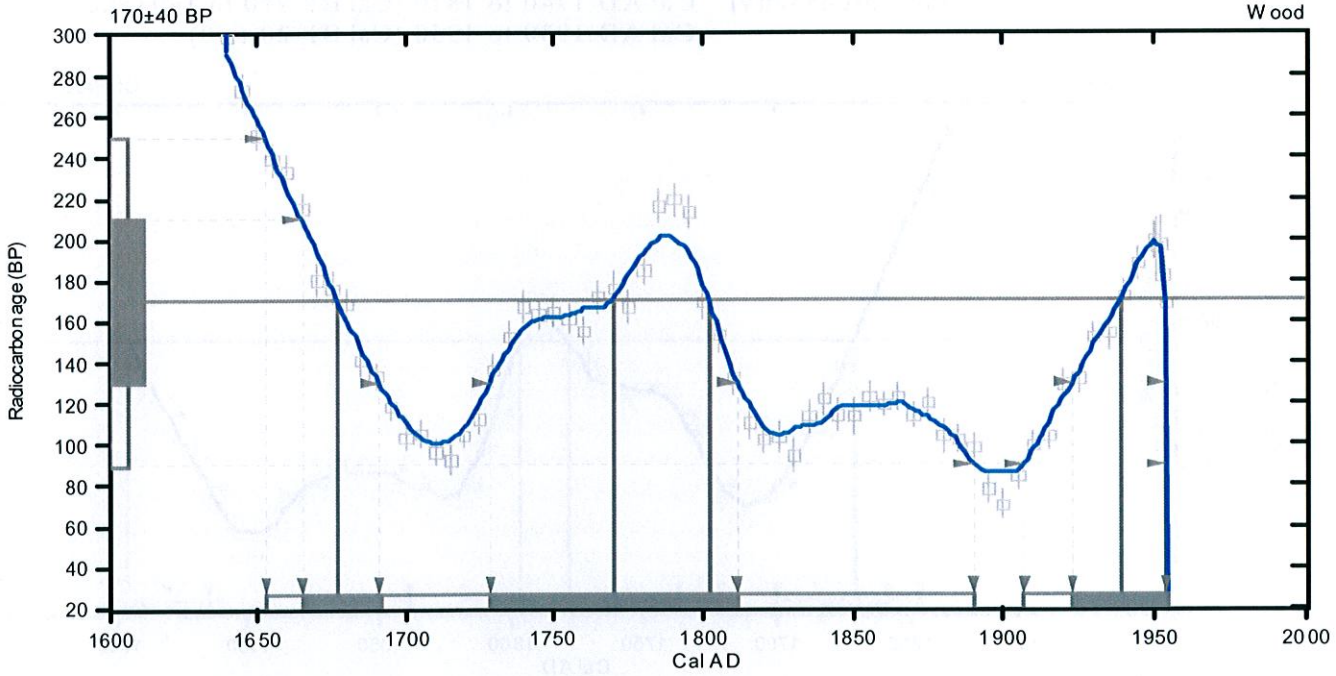

References:

Database used

INTCAL04

Calibration Database

INTCAL04 Radiocarbon Age Calibration

IntCal04: Calibration Issue of Radiocarbon (Volume 46, nr 3, 2004).

Mathematics

A Simplified Approach to Calibrating C14 Dates

Talma, A. S., Vogel, J. C., 1993, Radiocarbon 35(2), p317-322

Beta Analytic Radiocarbon Dating Laboratory

4985 S.W. 74th Court, Miami, Florida 33155 • Tel: (305)667-5167 • Fax: (305)663-0964 • E-Mail: beta@radiocarbon.com

CALIBRATION OF RADIOCARBON AGE TO CALENDAR YEARS

(Variables: C13/C12=-24.5:lab. mult=1)

Laboratory number: **Beta-242031**

Conventional radiocarbon age: **190±40 BP**

2 Sigma calibrated results: **Cal AD 1650 to 1700 (Cal BP 300 to 250) and**
(95% probability) **Cal AD 1720 to 1820 (Cal BP 230 to 130) and**
Cal AD 1840 to 1880 (Cal BP 110 to 70) and
Cal AD 1920 to 1950 (Cal BP 40 to 0)

Intercept data

Intercepts of radiocarbon age with calibration curve: Cal AD 1670 (Cal BP 280) and
Cal AD 1780 (Cal BP 170) and
Cal AD 1800 (Cal BP 150) and
Cal AD 1950 (Cal BP 0) and
Cal AD 1950 (Cal BP 0)

1 Sigma calibrated results: Cal AD 1660 to 1680 (Cal BP 290 to 270) and
(68% probability) Cal AD 1740 to 1810 (Cal BP 210 to 140) and
Cal AD 1930 to 1950 (Cal BP 20 to 0)

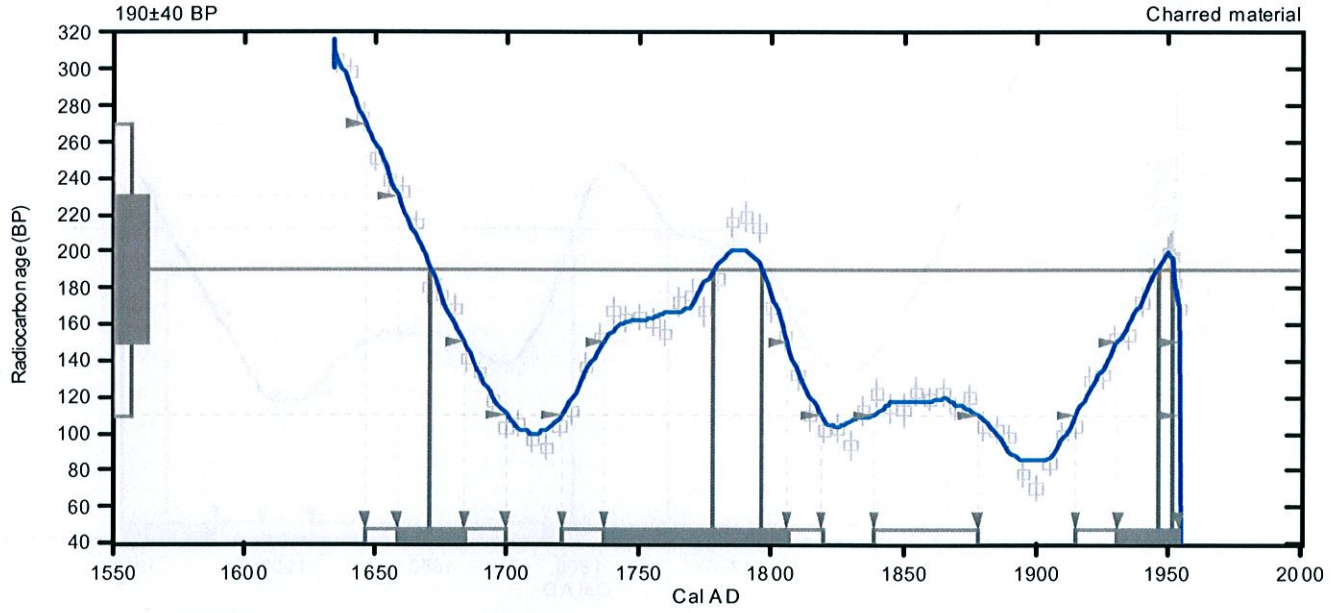

References:

Database used

INTCAL04

Calibration Database

INTCAL04 Radiocarbon Age Calibration

IntCal04: Calibration Issue of Radiocarbon (Volume 46, nr 3, 2004).

Mathematics

A Simplified Approach to Calibrating C14 Dates

Talma, A. S., Vogel, J. C., 1993, Radiocarbon 35(2), p317-322

Beta Analytic Radiocarbon Dating Laboratory

4985 S.W. 74th Court, Miami, Florida 33155 • Tel: (305)667-5167 • Fax: (305)663-0964 • E-Mail: beta@radiocarbon.com

Paleoseismological investigations of the Libna fault. Trench in Stari Grad.

Appendix 2

LMC Radiocarbon dating results

Laboratoire de Mesure du Carbone 14
UMS 2572 bâtiment 450 porte 4E
CEA Saclay, 91191 Gif sur Yvette Cedex

Préparation des échantillons : JP.Dumoulin

tel : 01 69 82 43 29
fax : 01 69 08 15 57
email : dumoulin@lsce.cnrs-gif.fr

Mesures et analyse des données : C.Moreau

tel : 01 69 08 14 05
fax : 01 69 08 15 57
email : christophe-r.moreau@cea.fr

Stéphane Baize -IRSN-
DEI/SARG CE FAR BP17
92262 Fontenay-aux-Roses

Saclay, le 02/08/2008

Cher Collègue,

Vous trouverez ci-après les résultats des mesures de concentration en ^{14}C de vos échantillons de matières organiques SG4, SG6 et SG7.

Les échantillons sont examinés à la loupe binoculaire afin d'éliminer d'éventuels contaminants (poils, fibres, radicelles…). Une quantité suffisante de l'échantillon est prélevée afin de procéder au traitement Acide, Base, Acide (A,B,A) :

- L'échantillon est traité à l'acide chlorhydrique 0.5N pendant 1 heure à 80°C afin d'éliminer les carbonates puis rincé à l'eau ultrapure jusqu'à pH neutre.
- L'échantillon est ensuite traité à la soude 0.1N pendant 1 heure à 80°C pour éliminer les acides humiques et fulviques. Le rinçage à l'eau ultrapure se poursuit jusqu'à pH neutre.
- L'échantillon subit un dernier lavage à HCl 0.5N pendant 1 heure à 80°C pour éliminer le CO_2 atmosphérique moderne éventuellement absorbé par l'échantillon lors du traitement basique. Le rinçage à l'eau ultrapure se poursuit jusqu'à pH neutre.

L'échantillon est séché dans une étuve à vide. Des quantités différentes selon la nature de l'échantillon sont prélevées afin d'obtenir, après combustion, un volume de CO_2 contenant environ 1 mg de C. L'échantillon est brûlé en présence d'environ 500 mg d'oxyde de cuivre et d'un fil d'argent pendant 4 heures à 900°C.

Le CO_2 obtenu est ensuite réduit par H_2 en présence de poudre de fer à 600°C. La quantité de fer est égale à 3 fois la quantité de carbone. Le carbone se dépose sur la poudre de fer et l'ensemble est ensuite pressé dans une cible.

L'activité en ^{14}C de l'échantillon est calculée en comparant les intensités mesurées séquentiellement des faisceaux de ^{14}C, ^{13}C et ^{12}C de chaque échantillon avec ceux de standards de CO_2 préparés à partir de l'acide oxalique de référence HOxI. Elle est exprimée en pMC (percent modern carbon) normalisé à un $\delta^{13}C$ de -25 pour mille. Les âges radiocarbone sont calculés selon Mook et Van der Plicht (Radiocarbon 41 (1999) p.227) en corrigeant le fractionnement avec le $\delta^{13}C$ calculé à partir de la mesure du rapport $^{13}C/^{12}C$ mesuré sur Artemis. Ce $\delta^{13}C$ inclut le fractionnement survenant aussi bien pendant la préparation des échantillons que pendant la mesure SMA. Il ne peut donc pas être comparé au $\delta^{13}C$ mesuré sur un spectromètre de masse. L'erreur sur la mesure tient compte à la fois de l'erreur statistique, de la variabilité des résultats et du blanc soustrait au résultat. Le résultat est donné sans soustraction d'âge réservoir.

Nous restons à votre disposition pour tout renseignement complémentaire concernant vos résultats.

Cordialement

Jean Pascal Dumoulin & Christophe Moreau

N° cible	référence échantillon	nature	mg C	$\delta^{13}C$	pMC corrigé du fractionnement			âge radiocarbone BP		
SacA 10343	SG4	MO	1.38	-26.00	97.25	±	0.19	225	±	30
SacA 10344	SG6	MO	1.23	-24.00	36.36	±	0.14	8125	±	30
SacA 10345	SG7	MO	0.72	-26.00	95.20	±	0.19	395	±	30

Paleoseismological investigations of the Libna fault. Trench in Stari Grad.

Appendix 3

OSL dating results

Institut für Geologie, Baltzerstrasse 1-3, CH-3012 Bern

Dr. Milos Bavec
Geological Survey of Slovenia
Dimieeva ulica 14
Ljubljana 1000
Slovenia

b
UNIVERSITÄT
BERN

Institut für Geologie

Bern, den 14.8.2008

Dear Dr Bavec,

Please find attached the results and interpretation of luminescence dating of two samples from Slovenia (samples SG-2 and SG-3).

If there any questions with regard to methodological issues or the interpretation of the results please don't hesitate to contact me.

Kind regards,

Frank Preusser

PD Dr. Frank Preusser

Baltzerstrase 1-3
CH-3012 Bern
Switzerland

Tel. +41 (0) 31 631 87 70
Fax +41 (0) 31 631 48 43
preusser@geo.unibe.ch
www.geo.unibe.ch

b
UNIVERSITÄT
BERN

Luminescence dating of samples SG-2 and SG-3

Methodology

Samples for luminescence dating were sent to our laboratory in opaque metal tubes together with additional material for dosimetry in normal plastic bags. After drying and determining moisture content, the latter material has been used for the determination of dose rate relevant elements (K, Th, U) using low-level high-resolution gamma spectrometry (cf. Preusser and Kasper 2001). The metal tubes were opened under subdued laboratory red-light conditions and the outer parts were removed due to possible light contamination. Material from the inner part of the tubes was treated with 10 % HCl and 30 % H_2O_2 to removed carbonates and organic matter. The grain-size 150-200 µm was gained by sieving. Subsequently, quartz and K-feldspar separates were isolated using heavy liquids. The quartz fraction was etched in 40 % HF for 60 min with subsequent treatment in 20 % HCl to remove fluorides.

Determination of the equivalent dose (ED) was carried out using the single-aliquot regenerative dose (SAR) protocol of Murray and Wintle (2000, 2003). Prior to ED determination standard test have been carried out to check the performance of the procedure (cf. Wintle and Murray 2006). For quartz, preheating at 230°C for 10 s was applied, while feldspar samples were preheated at 290°C for 10 s. Quartz Optically stimulated luminescence (OSL) was recorded during a 60 s exposure to blue diodes at 125°C samples temperature. Detection filter was a Hoya U340. For the K-feldspar samples, Infrared Stimulated Luminescence (IRSL) was recorded during a 300 s exposure to IR diodes at room temperature using a L.O.T. Oriel 410 nm interference filter combined with a Schott BG 39.

IRSL ages were determined using ADELE software (Kuhilg 2005) using present day depth and geographical location for calculation of cosmic dose rate and assuming that average sediment moisture during burial has been between 15-25 %.

Results and interpretation

The signal level of the quartz samples was too low to get any reliable ED estimates. The age interpretation is hence based on IRSL data only. The IRSL ages are 920 ± 1560 yr and 850 ± 190 yr. Considering the large error of SG2F and further possible uncertainties related to partial bleaching of the samples, we interpret that the sediment should be considered sub-modern, maybe of medieval age. It should be mentioned here that both samples are at the lower dating limit of the method.

References

Kulig, G. 2005. Erstellung einer Auswertesoftware zur Altersbestimmung mittels Lumineszenzverfahren unter spezieller Berücksichtigung des Einflusses radioaktiver Ungleichgewichte in der 238U-Zerfallsreihe. Unpublished BSc thesis, Technical University Bergakademie Freiberg.

Murray, A. S., Wintle, A.G., 2000. Luminescence dating of quartz using an improved single-aliquot regenerative-dose protocol. Radiation Measurements 32, 57-73.

Murray, A.S., Wintle, A.G., 2003. The single aliquot regenerative dose protocol: potential for improvements in reliability. Radiation Measurements 37, 377-381.

Preusser, F., Kasper, H.U. 2001. Comparison of dose rate determination using high-resolution gamma spectrometry and inductively coupled plasma - mass spectrometry. Ancient TL 19, 19-23.

Wintle, A., Murray, A.S. 2006. A review of quartz optically stimulated luminescence characteristics and their relevance in single-aliquot regeneration dating protocols. Radiation Measurements 41, 369-391.

Table 1. Summary data for luminescence dating giving: n = number of replicate measurements for quartz and polymineral fine-grain samples; K, Th, U = dose rate relevant elements; sediment moisture and depth below surface; dose rate (D), equivalent dose (ED) and age for both quartz (Q) and feldspar (F).

Sample	Grain size. (µm)	n	K (%)	Th (ppm)	U (ppm)	Moisture (%)	Depth (cm)	D-Q (Gy ka^{-1})	D-F (Gy ka^{-1})	ED-Q (Gy)	ED-F (Gy)	Age-Q (ka)	Age-F (ka)
SG2	150-200	-/27	1.02 ± 0.02	5.67 ± 0.24	1.63 ± 0.34	14.5	120	-	2.28 ± 0.30	-	2.1 ± 3.6	-	0.92 ± 1.56
SG3	150-200	-/24	0.98 ± 0.02	5.44 ± 0.11	2.62 ± 0.50	18.8	100	-	2.24 ± 0.17	-	1.9 ± 0.4	-	0.85 ± 0.19

Paleoseismological investigations of the Libna fault. Trench in Stari Grad.

Appendix 4

Paleontological analyses (sample SG 8)

HRVATSKI GEOLOŠKI INSTITUT - CROATIAN GEOLOGICAL SURVI

HRVATSKI GEOLOŠKI INSTITUT
CROATIAN GEOLOGICAL SURVEY
Zavod za geologiju / Department of Geology

Sachsova 2, P.O.Box 268, HR-10001 Zagreb, Croatia
Phone: (+385)-1-6160-888; Fax: (+385)-1-6144-718; MB 3219518
e-mail:ured@hgi-cgs.hr

Dr. sc. Valentina Hajek-Tadesse, dipl.ing.geol.

MIKROPALEONTOLOŠKE ANALIZE UZORAKA OKOLICE KRŠKOG

Broj: 56/08.

RAVNATELJ
dr. sc. Josip Halamić, dipl. ing. geol

PREDSTOJNIK
dr. sc. Ivan Hećimović, dipl. ing.geol

HRVATSKI GEOLOŠKI INSTITUT
ZAGREB - Sachsova 2

Zagreb, svibanj 2008

1) UVOD

U okviru projekta **„NSRAO, Krško“** za naručioca posla Geološki zavod Slovenije, izvršena je analiza ostrakodne faune pet uzoraka. Uzorci su laboratorijski pripremljeni u Sloveniji, a kabinetski dio posla od izdvajanja faune do determinacije izvršen je u Hrvatskom geološkom institutu u Zagrebu.

Prema priloženim podacima uz dostavljene uzorke, dva uzorka VGL-P3/1 (25,0-25,2 m) i VGL-P3/2 (28,8-29,9m) uzorkovana su iz plitkih bušotina na lokaciji Vrbina Gornji Lenart. Druga dva uzorka s oznakama BT-2 i BT-3 uzrokovana su na Brežiškoj terasi, a uzorak SG-8 u paleoseizmološkom jarku na lokaciji Stari Grad. Uz dostavljene podatke o lokacijama naručilac mikropaleontoloških analiza priložio je i predviđenu starost uzoraka (vidi tekst s opisom ostrakodne faune).

Prilikom determinacije ostrakodne faune korištena je paleontološka sistematika prema slijedećim autorima: Van Morkhoven (1962), Zanina i Polenova (1960), Krstić (1968), Sokač (1972,1989) i Meisch (2000).

2) PROMJENE U PODJELI GORNJOMIOCENSKIH NASLAGA PANONSKOG BAZENA

Do sada korištena podjela gornjeg miocena na katove Panon i Pont u prostoru Panonskog bazena više se ne koristi. U ovom izvještaju korištena je nova prihvaćena regionalna podjele gornjomiocenskih naslaga (sl.1).

U najnovijem radu Piller et al. (2007) uvode promjene koje se posebno ističu u kronostratigrafskoj shemi gornjeg miocena. Uzimajući u obzir sve dostupne podatke granica Sarmat / Panon se jasno korelira s granicom Seravalijan / Torton (srednji /gornji miocen). Početak donjeg Panona podudara se s TB 3.1, a gornji Panon s TB 3.2 i TB 3.3 (Haq et al. 1988). Kat Pont pripada u drugi geodinamski prostor i potpuno je isključen iz Panonskog bazenskog sistema. Isključivanje Ponta nije ishitren čin nego višegodišnji rad austrijskih, slovačkih i mađarskih stratigrafa.

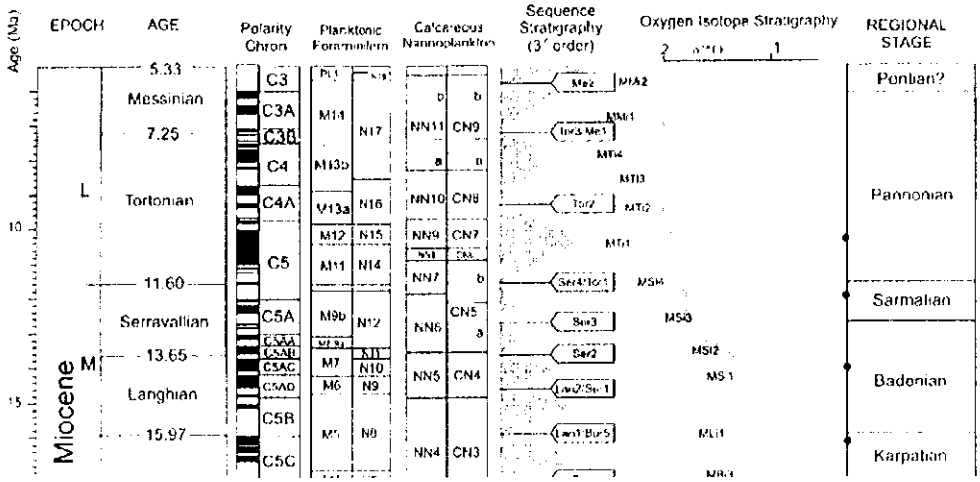

Sl.1 Prihvaćena podjela gornjeg miocena utemeljena na kompilaciji svih dostupnih podataka (Piller et al. 2007).

3) POPIS ANALIZIRANIH UZORAKA S DETERMINIRANOM OSTRAKODNOM FAUNOM

BT-2

Bacunella abchazica VEKULA
Candona (*Candoniella*) sp.
Candona (*Caspiolla*) sp.
Candona (*Lineocypris*) *granulosa* (ZALÁNYI)
Cyprideis triangulata KRSTIĆ
Hemicytheria croatica SOKAČ

Predviđena starost: sarmat ili pont.
S t a r o s t u z o r k a: **gornji panon,** zajednica *Cyprideis*-a.

BT-3

Amplocypris angulata (ZALÁNYI) (pretaložena)
Amplocypris cf. *major* KRSTIĆ
Candona (*Camptocypria*) *flectimarginata* SOKAČ
Candona (*Lineocypris*) *hodonensis* POKORNÝ
Candona (*Pontoniella*) *sagittosa* KRSTIĆ
Cypria sp.
Cyprideis cf *obesa* (REUSS)
Hemicytheria folliculosa (REUSS)
Leptocythere multituberculata (LIVENTAL)
Leptocythere naca (MÉHES)
Loxoconcha rhombovalis POKORNÝ
Loxoconcha sp.

+ mikromolusci i mikrogastropodi

Predviđena starost: sarmat ili pont.
S t a r o s t u z o r k a: **viši dio srednjeg panona,** zajednica *Camptocypria- Cyprideis-a.*

SG-8

Candona (*Lineocypris*) *hodonensis* POKORNÝ
Candona (*Typhlocypris*) cf. *eremita* (VEJDOVSKY)
Cyprideis cf *obesa* (REUSS)
Hemicytheria folliculosa (REUSS)
Hungarocypris marginata (ZALÁNYI)

Orygoceras sp.
+ krhotine mikromolusaka

Predviđena starost: sarmat.
S t a r o s t u z o r k a: **prijelaz donji panon /srednji panon** (C/D zona), zajednica *Hungarocypris*-a.

VGL – P 3/1 (25,0-25,2 m)

Candona (*Caspiolla*) *lobata* (ZALÁNYI)
Candona (*Typhlocypris*) cf. *eremita* (VEJDOVSKY)
Cyprideis sp.

+ mikromolusci i mikrogastropodi

Predviđena starost: pont.
S t a r o s t u z o r k a: **srednji panon,** zajednica *Caspiolla.*

VGL – P 3/2 (28,8-29,9m)

Candona (*Caspiocypris*) *lobiata* (ZALÁNYI)
Candona (*Caspiolla*) *lobata* (ZALÁNYI)
Candona (*Typhlocypris*) *eremita* (VEJDOVSKY)
Cypria tocorjescui HANGANU
Hemicytheria sp.
Leptocythere andrusovi (LIVENTAL)

Predviđena starost: pont.
S t a r o s t u z o r k a: **srednji panon,** zajednica *Caspiolla.*

4) PREGLED REZULTATA

Determinacija ostrakodne zajednice analiziranih uzoraka dala je zadovoljavajuće biostratigrafske rezultate. Prezentacija dobivenih rezultata uklopljena je u novu podjelu gornjemiocenskih naslaga Panonskog bazena.

Prijašnjih godina na našim prostorima bila je uvriježena podjela gornjeg miocena na dva kata: Panon i Pont. Kako je takva podjela „izbačena" iz prostora Panonskog bazena, uvedena je jednodijelna podjela gornjemiocenskih naslaga, tj. samo panonski kat koji je podijeljen na donji, srednji i gornji s pripadajućim Pappovim zonama.

Prihvaćanjem nove podjele olakšava se korelacija panonskih naslaga šireg prostora. Sve dosadašnje arhivirane podatke o starosti gornjomiocenskih naslaga kod buduće upotrebe ili publikacije potrebno je preimenovati prema važećim kriterijima.

Analizirani ostrakodi pripadaju podredu P o d o c o p a odnosno familijama *Cyprididae* i *Cytheridae*. Većina vrsta određena je pouzdano. Ukupno je određeno deset rodova i dvadesetipet ostrakodnih vrsta. Uz ljušturice ostrakoda koje su i najbrojnije, u uzorcima se nalaze mikromolusci i mikrogastropodi. Osim odredbe starosti zbog dominacije pojedinih rodova određene su i ostrakodne zajednice tipične za svaki uzorak. Izdvojene zajednice su rezultat promjenjivih paleoekoloških uvjeta u panonskom jezeru.

Najstarija ostrakodna fauna određena je u uzorku BS-8, u kojemu dominira zajednica *Hungarocypris-a.* Iako je predviđena starost naslaga bila sarmat, u uzorku je određena panonska starost naslaga i to najviši dio donjeg panona ili najniži dio srednjeg panona, (prijelaz Pappove zone C- D).

Napomena: U prijašnjim izvještajima ostrakodna fauna pripadala bi istoj zoni, ali bi starost naslaga bila određena kao gornjepanonska.

U uzorcima BT-2 i BT-3 uzorkovanim na Brežiškoj terasi, za koje je bila pretpostavljena sarmatska ili pontska starost, određena je za uzorak B-3 srednjepanonska starost-viši dio, te za uzorak B-2: gornje panonska starost naslaga (zona F). U uzorku B-2 dominira rod *Cyprideis,* a u uzorku B-3 zajednica *Camptocypria- Cyprideis.*

Napomena: U prijašnjim izvještajima temeljem navedene ostrakodne zajednice u oba uzorka bila bi određena pontska starost.

Uzorci uzeti iz plitkih bušotina u Vrbini, Gornji Lenart VGL–P3/1 (25,0-25,2 m) i VGL–P 3/2 (28,8-29,9m) pretpostavljene su pontske starosti. Analizom ostrakodne zajednice, koja je slična u oba uzorka ali raznolikija vrstama u uzorku VGL-P3/2, određena je srednjepanonska starost.

Napomena: U prijašnjim izvještajima ostrakodna fauna bila bi pontske strosti.

U svim uzorcima su zastupljeni plitkovodni i dubljevodniji oblici. Nalaz vrsta: *Cyprideis triangulata, Cyprideis* cf. *obesa, Hemicytheria croatica, Hemicytheria folliculosa, Leptocythere multituberculata, Leptocythere naca, Loxoconcha rhombovalis, Loxoconcha* sp. i *Leptocythere andrusovi* ukazuju na povećani salinitet vode, odnosno na oligohalinsko do mezohalinsku vodenu sredinu.

Ostrakodna zajednica je autohtona, izuzev dijela faune u uzorku BT-3, gdje se uz autohtonu faunu nalazi i pokoja starije panonska pretaložena ostrakodna ljušturica.

5) POPIS LITERATURE

HAQ, B. U., HARDENBOL, J. & VAIL, P.R.(1988): Mesozoic and Cenozoic chronostratigraphy and cycles of sea level changes. In: Wilgus, C. K., Ed., *Sea –level changes-an integrated approach*,71-108. Society of Economic Paleontologists and Mineralogists, Special Publications, 42.

KRSTIĆ, N. (1968): Biostratigrafija, taksonomija i filogenija Cypridida (Ostr.) kongerijskih slojevaokoline Beograda, *Doctoral dissertation*, p.1-366, pl.I-LXXVIII, Rudarsko-geološki fakultet, Beograd.

MEISCH, C. (2000): Freshwater Ostracoda of Western and Central Europe. *Spektrum Akademisher Verlag*. 1-515.

MORKHOVEN, F. P. C. M. VAN (1962): Post – Palaeozoic Ostracoda. Their Morphology, Taxonomy and Economic Use. Vol.I, General. P.1-204; Amsterdam / London / NewYork (Elsevier Publ.Co).

PILLER, W. E., HARZHAUSER, M. & MANDIĆ, O. (2007): Miocene Central Paratethys stratigraphy - current status and future directions. *Stratigraphy,* vol.4., 151-168.

SOKAČ, A. (1972): Pannonian and Pontian Ostracode Fauna of Mt. Medvednica, *Paleont. jugosl. Jugosl. Akad.*, 11: 9-140, 47 pls., 3 figs.,1 map, Zagreb.

SOKAČ, A. (1989): Pontian ostracod fauna in the Pannonian Basin. *Chronostratigraphie und Neostratotypen , Pliozän Pl , Pontien.* JAZU,SANU; Zagreb-Beograd,672-722.

ZANINA, I. N. & POLENOVA, E. N. (1969): Podklass Osracoda. Osnovy paleontologiii. Členistogie, trilobitoobraznye i rakoobraznye, p.264-421, Moskva.

Paleoseismological investigations of the Libna fault. Trench in Stari Grad.

Appendix 5

Geophysical preliminaries for trench siting

GEOINŽENIRING d.o.o.
Geotehnične, geološke in geofizikalne raziskave, projektiranje, svetovanje in inženiring

POSKUSNE GEOFIZIKALNE PREISKAVE ZA UGOTAVLJANJE LOKACIJE LIBENSKEGA PRELOMA PRI KRŠKEM

Preliminarno poročilo

Arhiv.št.:	GF-1280
D.N.	40-XXXX/2008
Datum:	januar 2008
Obdelala:	Robert Stopar, *univ.dipl.ing.geol.*
	Marjeta Car, *univ.dipl. ing. geol.*
Pregledala:	Marjeta Car, *univ.dipl. ing. geol.*
Direktor:	Boris Rijavec, *univ.dipl.ing.grad.*

OSNOVNI PODATKI

1.	Naslov poročila:	POSKUSNA GEOFIZIKALNE PREISKAVE ZA UGOTAVLJANJE LOKACIJE LIBENSKEGA PRELOMA PRI KRŠKEM
2.	Številka poročila:	GF-1280
3.	Gesla:	seizmika, refrakcija, MASW, georadar, prelom, Libenski prelom, Krško
4.	Obseg poročila:	III + 10 strani, 3 priloge;
5.	Naloga raziskav:	pridobiti dodatne informacije za lociranje geološkega izkopa za ugotavljanje poteka Libenskega preloma
6.	Investitor:	ARAO in GEN energija
7.	Pogodba in delovni nalog:	DN 40-XXXX/08
8.	Lokacija raziskav:	Krško, Libna x1 = 540749 x2 = 540935 y1 = 89197 y2 = 89314
9.	Obseg del:	9 seizmičnih refr. profilov (skupaj 224 m, d=1m), aktivni MASW (65 MASW točk)
10.	Čas terenskih /laboratorijskih del:	januar 2008
11.	Nosilec naloge:	Marjeta Car, univ.dipl.ing.geol.
12.	Obdelava in poročilo:	Marjeta Car, univ.dipl.ing.geol. Robert Stopar, univ.dipl.ing.geol.
13.	Terenske meritve:	Ivan Majhen, ing. geot. Rudi Štiglic, elek. tehn. Sandi Kmetič, geol. tehn.
14.	Grafična oprema:	Sandi Kmetič, geol. tehn.
15.	Poročilo izdelano:	19. januar 2008

KRATKA VSEBINA

Preliminarno poročilo o poskusnih geofizikalnih preiskavah na območju, kjer je predviden geološki izkop za ugotavljanje lokacije Libenskega preloma, vsebujejo zgolj seizmične preiskave. Georadarske preiskave so predvidene za naslednjo fazo preiskav, ko bodo razmere na terenu bolj ugoden (sušno obdobje). Rezultati seizmičnih profilov, ki so bili izdelani z meotodama plitve refrakcijske seizmike oziroma MASW, ne kažejo na prisotnost večjih anomalij. Seizmične hitrosti so razmeroma enakomerno porazdeljene. Opazna je poglobitev na območju dvignjene terase in rahle nepravilnosti v globljih plasteh, ki sicer odstopajo od okolice, a ni nujno, da odražajo (samo) prisotnost prelomne cone.

VSEBINA

stran

PRILOGE

1. UVOD

Geoinženiring d.o.o. je na osnovi dogovora med predstavniki naročnikov (Agencija za radioaktivne odpadke RS in GEN energija Krško), predstavniki Geološkega zavoda ter predstavnikom Geoinženiringa d.o.o. izvedel poskusne geofizikalne preiskave na ožjem območju južno od vasi Libna pri Krškem. Glavni namen poskusnih geofizikalnih preiskav je bil ugotoviti anomalije v fizikalnih lastnostih sedimentov plitvo pod površjem, ki bi lahko kazale na možnost obstoja Libenskega preloma oziroma prelomne cone. Lokacijo preiskav so predhodno podali geologi iz Geološkega zavoda Slovenije. Za reševanje take problematike ne obstaja nobena res ustrezna površinska geofizikalna metoda. Odločili smo se za dve metodi, ki imata primerne predispozicije za ugotavljanje anomalij, ki bi jih posredno lahko povezovali s tektoniko : plitvo seizmično profiliranje (refrakcija in MASW) ter georadarsko profiliranje. Seveda pa obstaja tudi možnost, da kontrastnosti ne bo. Uporabniki geofizikalnih rezultatov se strinjajo, da kljub sorazmerno velikem tveganju za uspešnost geofizikalnih preiskav, le-te izvedemo, saj so pričakovane prednosti v primeru uspešnosti večje kot mikrolociranje raziskovalnega razkopa brez geofizikalnih podatkov.

Ker je bilo v času pred pričetkom geofizikalnih meritev deževno obdobje in so bila tla razmeroma močno razmočena, georadarskih preiskav v tem času nismo izvedli. Zato georadarske preiskave niso zajete v preliminarnem poročilu.

2. TEHNIČNI PODATKI

Geofizikalne preiskave smo zasnovali v skladu z zahtevami naročnika in možnostmi posamezne metode. Zaradi razmeroma kratkega časovnega roka, ki je vezan na izvedbo geološkega izkopa na preiskovanem območju, smo menili, da so najprimernejše geofizikalne metode za izpolnitev zastavljene naloge plitva refrakcijska seizmika, aktivna MASW (Mulichannel Analysis of Surface Waves) metoda ter georadarska metoda, ki omogočajo razmeroma hitro in enostavno izvedbo. Vse geofizikalne meritve so potekale vzdolž profila, ki ga je predlagal Geološki zavod Slovenije. Pred geofizikalnimi meritvami profil ni bil geodetsko posnet. Za lociranje profila v naravi smo uporabili orto-foto posnetek v merilu 1:500, ki ga podajamo na

prilogi 1. Referenčne točke smo označili z oznakami od S01 do S09.

Seizmični refrakcijski profil je sestavljen iz 9 krajših razvrstitev, ki imajo središčne točke na omenjenih referenčnih točkah. Vzdolž celotnega profila je bilo skupaj 216 sprejemnikov seizmičnega signala ali geofonov, ki so bili med seboj v razmaku 1 m. Strelne točke, na katerih smo s pomočjo kladiva mase 8 kg prožili seizmično valovanje, so bile simetrično razporejene vzdolž profila. Geometrija merskih in strelnih točk je omogočala zajem podatkov do globine okoli 15 m ter razmeroma dobro resolucijo (vsaj 1 m). Seizmični signal smo registrirali in posneli na seizmografu ABEM Terraloc Mk6 v lasti Geološkega zavoda Slovenije. Razmerje med seizmičnim signalom in šumom je bil večinoma dober, kar je razvidno na sliki 1.

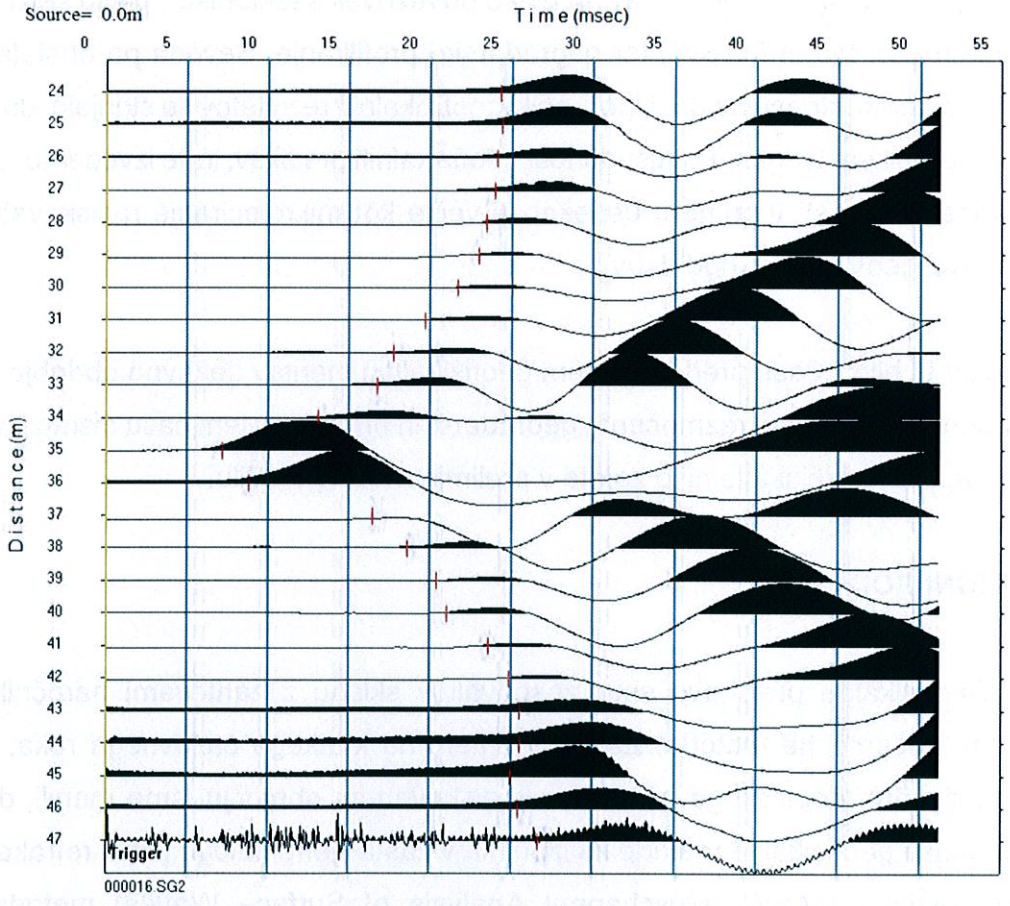

Slika 1. Seizmični posnetek in odčitani prvi prihodi pri refrakcijski seizmiki

Vzdolž geofizikalnega profila smo izmerili tudi 65 MASW (Multichannel Analysis of Surface Waves) točk v medsebojnem razmaku (offset) 3 m. Uporabili smo t.i. aktivno MASW metodo plitvega dosega (do 15 m). Za vzbujanje površinskih valov smo uporabili kladivo mase 8 kg. Osnovni podatki o MASW meritvah so podani v tabeli 1.

Parameter	Nastavitev
Razvrstitev	linijska
Dolžina razvrstitve	24 m
Razdalja med sprejemniki	1 m
Število sprejemnikov	24
Tip sprejemnika	4,5 Hz vertikalni geofon
Položaj strela (offset)	3 m od 1. geofona
Seizmični vir	Kladivo 8 kg
Vzorčevanje	0,5 msek.
Dolžina posnetka	1,6 sek.
Število posnetkov	10 posnetkov (stacking)

TABELA 1. Osnovni podatki o meritvah z aktivno MASW metodo na posamezni točki

Sprejemniki ali geofoni so bili zaradi enostavnejših in hitrejših meritev pritrjeni na poseben tračni sistem (landstreamer), ki smo ga izdelali na Geoinženiringu d.o.o. Na slikah 2a in 2b je prikazan način meritve neposredno na terenu.

Slika 2a Tračni sistem geofonov ali "landstreamer"

Slika 2b Potek seizmičnih meritev

Razmerje med seizmičnim signalom in šumom je bilo pri MASW meritvah znatno slabše kot pri refrakcijskih, zato so te meritve nekoliko slabše kvalitete.

3. METODOLOGIJA GEOFIZIKALNIH PREISKAV

3.1. Refrakcijska seizmika

Metoda refrakcijske seizmike temelji na meritvah hitrosti širjenja seizmičnega valovanja skozi različne seizmično odzivne plasti. Meritve potekajo vzdolž profila, na katerem so v običajno pravilnem razmiku razvrščeni sprejemniki valovanja ali geofoni. Vzdolž profila prožimo seizmično energijo v različnih točkah, ki so navadno razporejene simetrično. Neposredno na terenu merimo čase prihodov seizmičnega valovanja do posameznih geofonov, ki nam predstavljajo merska mesta. Na t.i. seizmogramih lahko razberemo čase prvih prihodov, ki praviloma predstavljajo refraktirani val. Le-ta poteka od seizmičnega vira pod kritičnim kotom do kontakta dveh seizmično različnih medijev, potuje vzdolž kontakta in se nato ponovno pod kritičnim kotom odbije na površino, kjer ga zaznamo s sprejemnikom ali geofonom. Shemo in postopek refrakcijske tehnike prikazuje slika 3. Seizmični signal seveda vsebuje tudi motnje (šum), ki jih navadno odstranimo z različnimi postopki filtriranja signala.

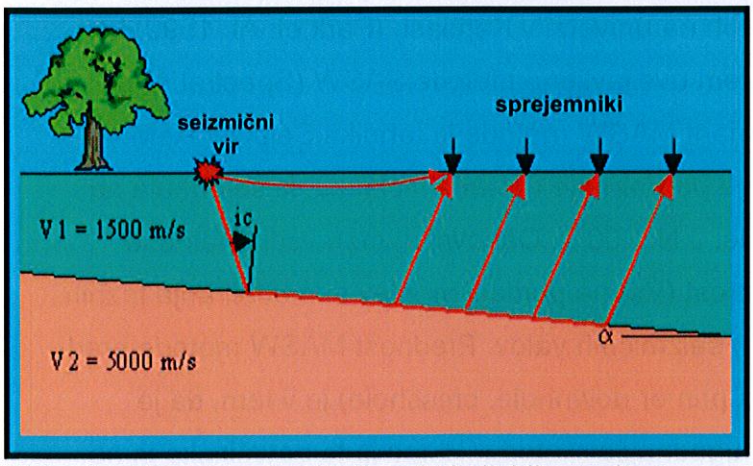

Slika 3. Shema seizmičnih refrakcijskih meritev

S pomočjo geometrije sprejemnikov in strelnih mest ter izmerjenimi časi prvih prihodov izračunamo hitrosti širjenja bodisi longitudinalnega ali transverzalnega valovanja skozi različne plasti ter z različnimi matematičnimi postopki tudi globine njihovih kontaktov.

Uspešnost metode je odvisna od odzivnosti posameznih plasti oziroma njihovega seizmičnega kontrasta, ki ga odraža predvsem gostota kamnine. Globinski doseg metode je močno odvisen od hitrosti medijev, ustrezne geometrije refrakcijske

razvrstitve in njene dolžine. Seizmična refrakcijska metoda je deloma omejena, ker temelji na predpostavki, da se hitrost širjenja valovanja veča z globino posameznih plasti. Za globinski doseg metode je torej pomemben pogoj v1<v2<v3 .... oziroma, da je hitrost globlje plasti večja od zgornje. Nekatere metode pa so neodvisne od omenjenega pogoja, na primer direktno modeliranje s pomočjo optimizacije (tomografija). Metoda temelji na postavitvi optimalnega modela in izračunu prvih prihodov v primerjavi z izmerjenimi časi prvih prihodov. To je iterativna metoda, ki zahteva zmogljivo računalniško podporo.

Praviloma odražajo višje seizmične hitrosti bolj trdno in kompaktno kamnino. Zemljine imajo večinoma nižje hitrosti, razen ob večji prisotnosti vode ali zasičenosti, ko so hitrosti P- valovanja prek 1500 m/s.

3.2. Aktivna MASW metoda

V novejšem času se za določitev in-situ elastičnih parametrov tal in trdnosti tal v potresnem inženirstvu in inženirski geofiziki nasploh vse bolj uveljavljajo t.i. metode površinskih seizmičnih valov. Metodo MASW (Multichannel Analysis of Surface Waves) so razvili v poznih 90-ih letih na univerzi v Kansasu (Park et. Al. 1999) kot nadaljevanje in izpopolnitev pred tem uveljavljene metode SASW (Spectral Analysis of Surface Waves). Ena izmed variant MASW metode je tehnika SeisOpt ReMi (Refraction Microtremor). Metoda je podrobneje opisana v članku, ki se nahaja na spletni strani Optim software (Louie, J.N. 2001). Osnovni namen vseh metod je določiti transverzalno ali strižno hitrost (Vs) na podlagi meritev in modeliranja faznih hitrosti površinskih (Rayleigh-jevih) seizmičnih valov. Prednost MASW metode pred ostalimi seizmičnimi metodami (na primer downhole, crosshole) je v tem, da je enostavnejša, hitrejša in cenovno ugodnejša metoda. Hkrati je to površinska in ne-destruktivna metoda.

MASW metoda se lahko izvaja na dva načina. Prvi način je t.i. aktivna MASW metoda, pri kateri površinsko valovanje vzbujamo z različnim seizmičnim virom (običajno kladivo) na določeni strelni točki, ki je običajno 10% - 20 % dolžine MASW

razvrstitve. Globinski doseg aktivne MASW metode je odvisen od dolžine razvrstitve. Običajno je manj kot 20 m. Osnovni princip aktivne MASW je prikazan na sliki 4.

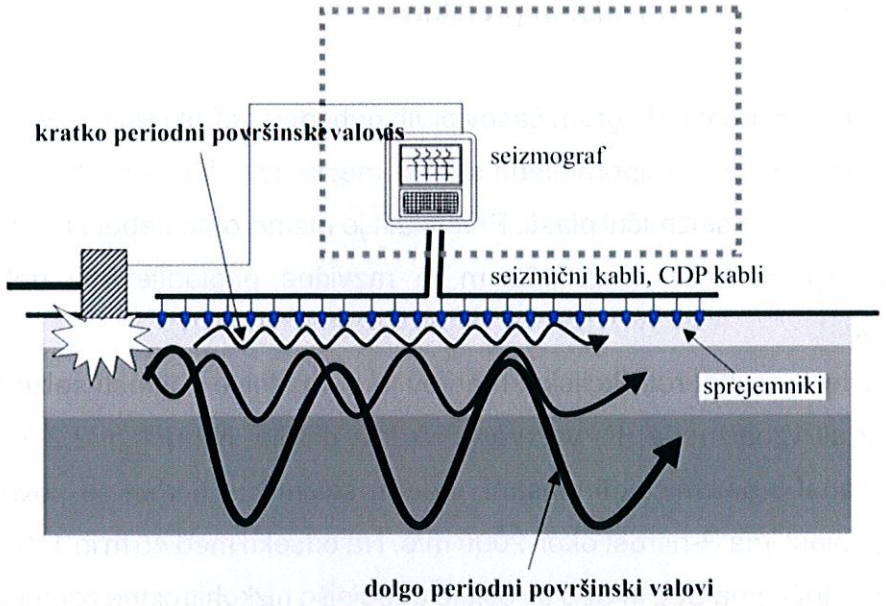

Slika 4. Princip aktivne MASW meritve

Značaj amplitudnega spektra površinskih valov je disperzijski. Iz diagrama faznih hitrosti-frekvenca je možno odčitati disperzijsko krivuljo. Hitrosti Rayleigh-jevih površinskih valov so neposredno povezane s strižnim valovanjem, tako lahko z inverznim modeliranjem disperzijske krivulje izračunamo hitrosti strižnega valovanja. Končni rezultat MASW meritev so 1D diagrami strižnih ali transverzalnih seizmičnih hitrosti, ki jih lahko združimo v enoten seizmični profil, če jih izvajamo zvezno vzdolž profila.

3.3. Georadarska metoda

Georadarske meritve niso zajete v preliminarnem poročilu.

4. REZULTATI GEOFIZIKALNIH PREISKAV

4.1. Rezultati seizmičnih refrakcijskih preiskav

Na prilogi 2.1 je podan diagram časov prvih prihodov (refrakcijskega valovanja) v odvisnosti od razdalje za vsa uporabljena strelna mesta. Iz naklona premic prihodov lahko razberemo vsaj dve seizmični plasti. Prva plast je razmeroma debela in ima nizke hitrosti. Na razdalji med 50 m in 100 m je razvidna poglobitev ali debelejša nizkohitrostna plast.

Neposreden rezultat refrakcijskih meritev je porazdelitev hitrosti seizmičnega *longitudinalnega* ali *vzdolžnega* (P) valovanja vzdolž profila. Na prilogi 2.2 je zgoraj prikazan grob model s seizmičnimi plastmi, katerih seizmična hitrost se povečuje z globino. Spodnja plast ima P-hitrost okoli 2000 m/s. Na odseku med 45 m in 110 m, to je med referenčnima točkama S02 in S05 so očitno debelejše nizkohitrostne zgornje plasti. Iz seizmičnega vidika so to »mehkejši« sedimenti. Možno je, da je to v povezavi s teraso, ki jo prečkamo v bližini točke S02. Zlasti med točkama S02 in S03 so opazne tudi rahle nepravilnosti v globljih plasteh (anomalije). Ali je to posledica možne prelomne cone samo s seizmičnimi podatki ne moremo zanesljivo potrditi. Analogne anomalije so razvidne tudi na osrednjem modelu (priloga 2.2), ki je bil izdelan s tomografsko tehniko.

4.2. Rezultati seizmičnih MASW preiskav

Rezultat MASW meritev je porazdelitev *transverzalnih* ali *strižnih* (S) seizmičnih hitrosti vzdolž profila. Značaj teh hitrosti je povsem drugačen od longitudinalnih in je neodvisen od zasičenosti kamnine z vodo. Na sliki 5 je prikazana disperzija površinskih valov z odčitano disperzijsko krivuljo.

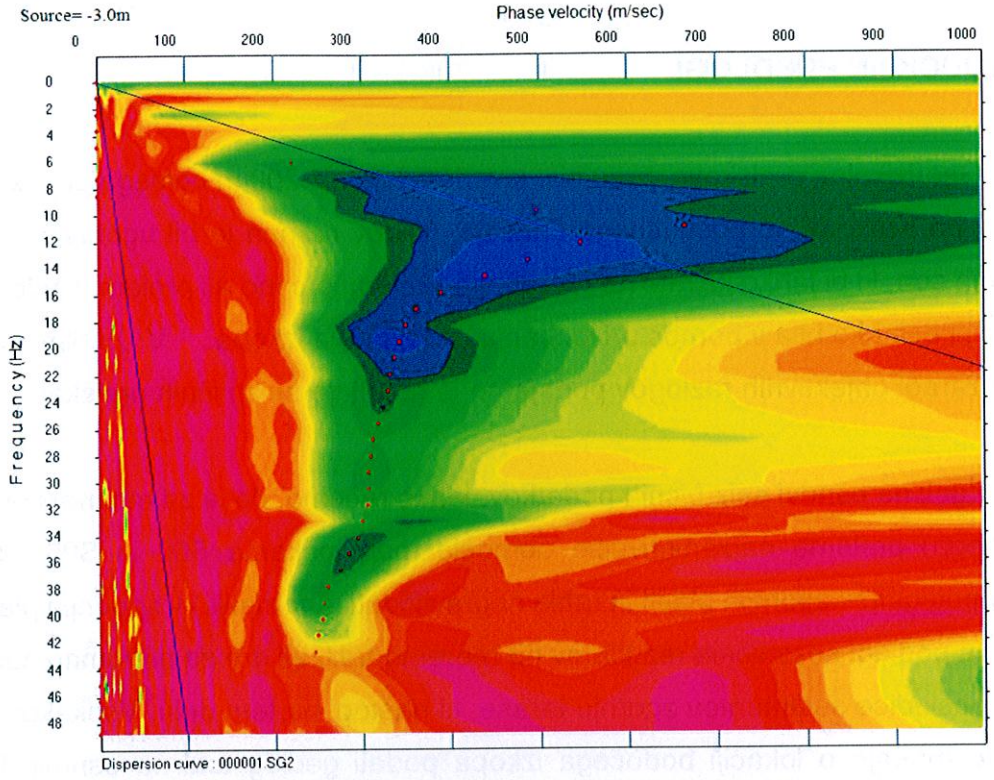

Slika 5. Diagram faznih hitrosti v odvisnosti od frekvence ter disperzijska krivulja na MASW točki

Seizmični profil, ki je bil izdelan s tehniko MASW, je podan na spodnjem profilu na prilogi 2.2. Na profilu so očitne nepravilne oblike, ki so najverjetneje posledica omenjene slabše kakovosti signala. Kljub temu je tudi na tem profilu očitna večja debelina zgornjih sedimentov med točkama S02 in S05 ter nepravilnosti v globljih plasteh. Poglobitev je tudi verjetno v okolici točke S09.

4.3. Rezultati georadarskih preiskav

Rezultati georadarskih meritve niso zajeti v preliminarnem poročilu.

5. ZAKLJUČKI IN PREDLOGI

Geofizikalne preiskave, ki so bile izvedene vzdolž 200 m dolgega profila južno od Libne pri Krškem, so poskusnega značaja. Njihov namen je bil ugotoviti lokacije anomalnih con, ki bi lahko kazale na morebitno prelomno cono ali prelom. Pridobljena informacija bi lahko bila v pomoč pri lociranju geološkega izkopa. V preliminarnem poročilu zaradi objektivnih razlogov podajamo le rezultate seizmičnih preiskav.

Zgolj na osnovi seizmičnih podatkov, lahko rečemo, da je za možnost obstoja (Libenskega) preloma najzanimivejše območje med točkama S02 in S05, kjer je največja poglobitev zgornjih plasti in rahle nepravilnosti (anomalije) v spodnjih plasteh. Vendar na podlagi seizmičnih rezultatov ne moremo trditi ali gre za prelomno cono ali zgolj za posledice sedimentov zgornje terase, ki nastopi na tem delu. Vsekakor mora dokončno mnenje o lokaciji bodočega izkopa podati geolog tudi na osnovi drugih podatkov. V nadaljevanju naloge pričakujemo tudi nekatere izsledke iz predvidenih georadarskih meritev na omenjenem geofizikalnem profilu

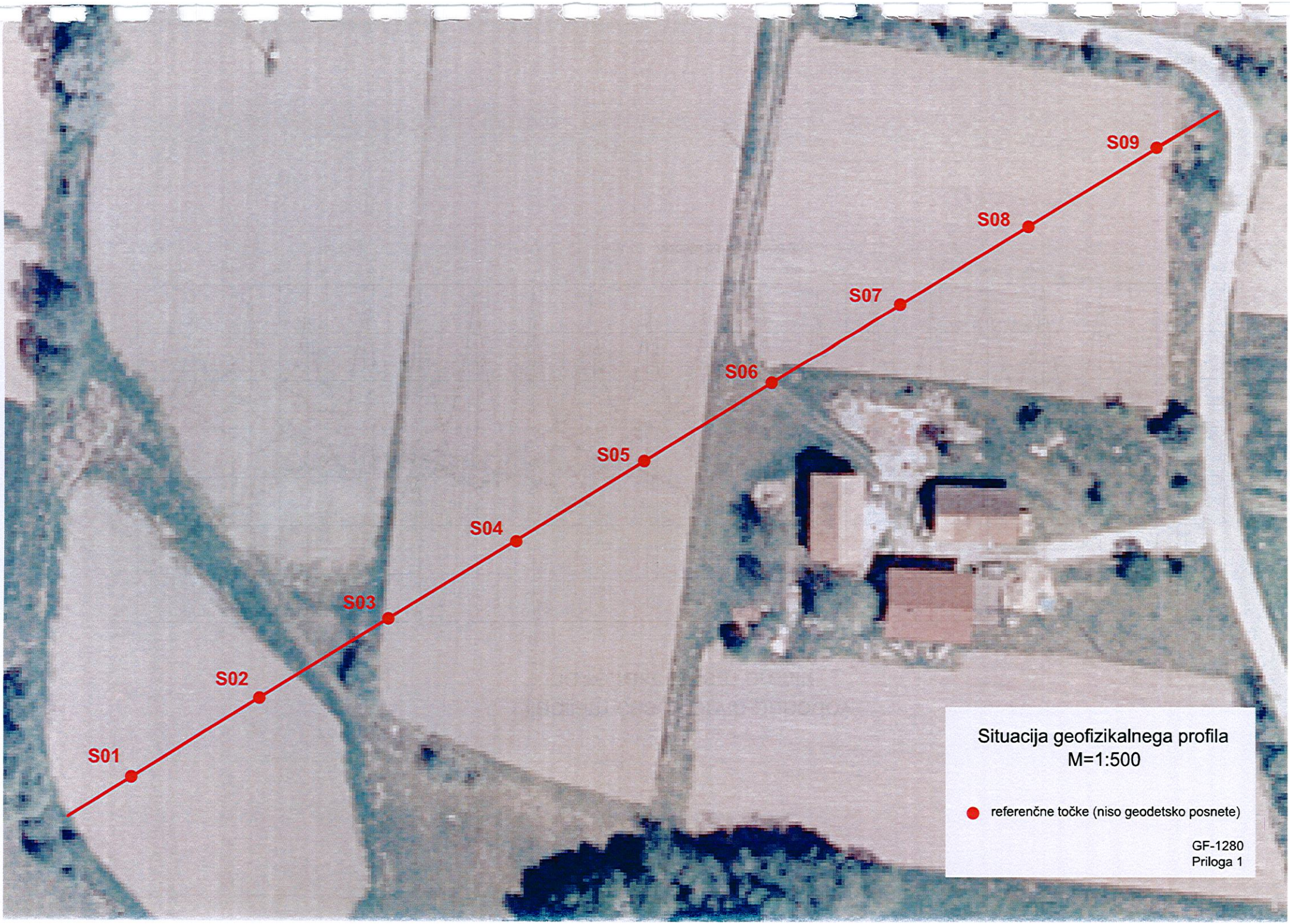
S01
S02
S03
S04
S05
S06
S07
S08
S09
Situacija geofizikalnega profila
M=1:500
referenčne točke (niso geodetsko posnete)
GF-1280
Priloga 1

Diagram časov prvih prihodov na refrakcijskem profilu

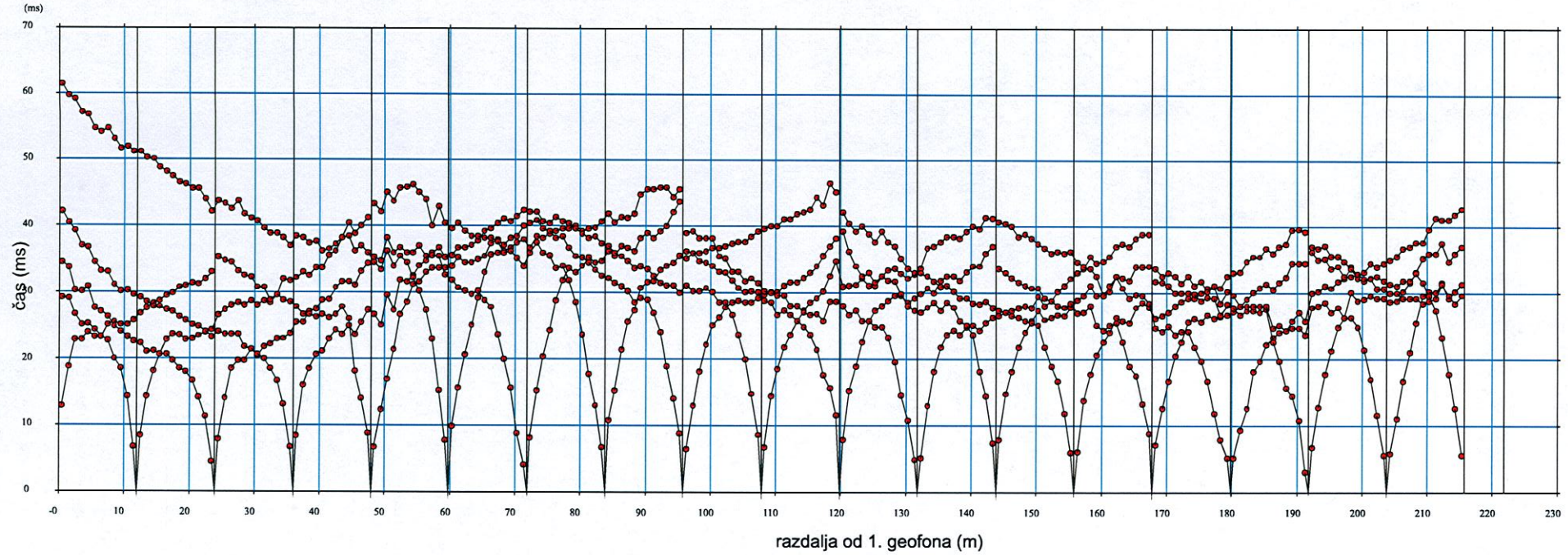

GF-1280
Priloga 2.1.

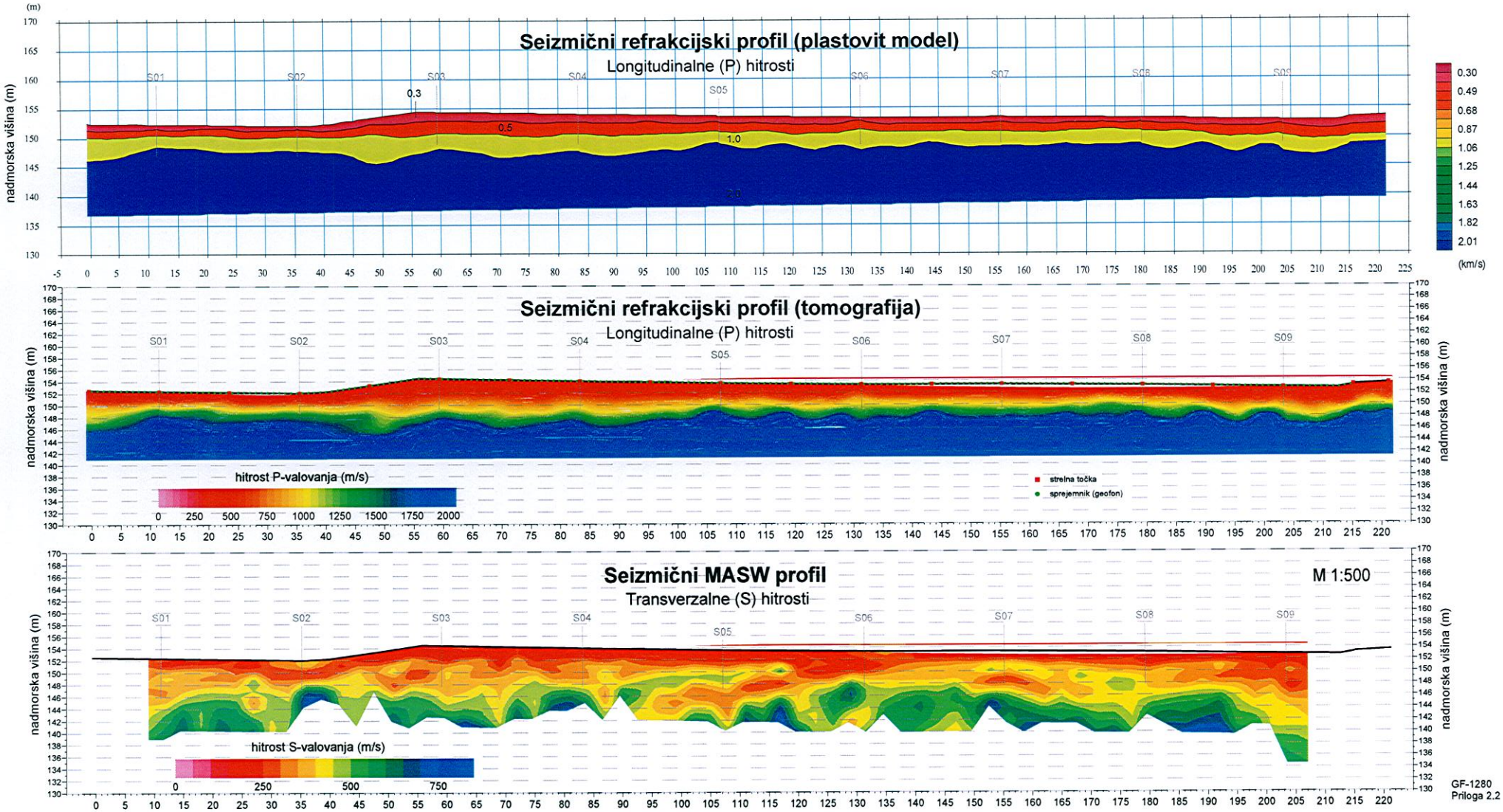

GF-1280
Priloga 2.2